

## Article

# Production and Characterization of a $\beta$ -Cyclodextrin Inclusion Complex with *Platonia insignis* Seed Extract as a Proposal for a Gastroprotective System

Juliana Lima Nascimento <sup>1</sup>, Angélica Gomes Coelho <sup>2</sup>, Ytallo Samuel Oliveira Barros <sup>1</sup>, Irisdalva Sousa Oliveira <sup>3</sup>, Francilene Vieira da Silva <sup>3</sup>, Ana Flávia Seraine Custódio Viana <sup>3</sup>, Bruno Quirino Araújo <sup>1</sup>, Márcio dos Santos Rocha <sup>1</sup>, Francisco das Chagas Pereira de Andrade <sup>2</sup> , Celma de Oliveira Barbosa <sup>2</sup>, Hélio de Barros Fernandes <sup>2</sup>, Anderson Nogueira Mendes <sup>2</sup> , Joaquim Soares da Costa-Júnior <sup>4</sup>, Rita de Cássia Meneses Oliveira <sup>2,3</sup>, Massimo Lucarini <sup>5</sup>, Alessandra Durazzo <sup>5,\*</sup> , Daniel Dias Rufino Arcanjo <sup>2,\*</sup>  and Antônia Maria das Graças Lopes Citó <sup>1</sup>

<sup>1</sup> Laboratório de Geoquímica Orgânica, LAGO, Universidade Federal do Piauí, Teresina, Piauí 64049-550, Brazil

<sup>2</sup> Departamento de Biofísica e Fisiologia, Universidade Federal do Piauí, Teresina, Piauí 64049-550, Brazil

<sup>3</sup> Núcleo de Pesquisas em Plantas Medicinais, NPPM, Universidade Federal do Piauí, Teresina, Piauí 64049-550, Brazil

<sup>4</sup> Departamento de Química, Instituto Federal de Educação, Ciência e Tecnologia do Piauí, Teresina, Piauí 64000-040, Brazil

<sup>5</sup> CREA—Research Centre for Food and Nutrition, 00178 Rome, Italy

\* Correspondence: alessandra.durazzo@crea.gov.it (A.D.); daniel.arcanjo@ufpi.edu.br (D.D.R.A.)



**Citation:** Lima Nascimento, J.; Coelho, A.G.; Oliveira Barros, Y.S.; Sousa Oliveira, I.; Vieira da Silva, F.; Custódio Viana, A.F.S.; Araújo, B.Q.; dos Santos Rocha, M.; das Chagas Pereira de Andrade, F.; de Oliveira Barbosa, C.; et al. Production and Characterization of a  $\beta$ -Cyclodextrin Inclusion Complex with *Platonia insignis* Seed Extract as a Proposal for a Gastroprotective System. *Appl. Sci.* **2023**, *13*, 58. <https://doi.org/10.3390/app13010058>

Academic Editor: Lionel Maurizi

Received: 25 October 2022

Revised: 13 December 2022

Accepted: 14 December 2022

Published: 21 December 2022



**Copyright:** © 2022 by the authors. Licensee MDPI, Basel, Switzerland. This article is an open access article distributed under the terms and conditions of the Creative Commons Attribution (CC BY) license (<https://creativecommons.org/licenses/by/4.0/>).

**Abstract:** *Platonia insignis* Mart, Clusiaceae, known as *bacuri*, is a species native to Brazil that, in studies with extract of the seed of its fruit, showed antioxidant activity against free radicals. Products with such properties may be of great importance in the treatment of peptic ulcers since this pathology may be associated with the inflammatory process caused by the action of free radicals. Cyclodextrins are molecules capable of forming inclusion complexes with other molecules, affecting their physicochemical properties and improving their pharmacokinetic characteristics. Thus, this work aimed to produce, characterize, and evaluate the gastroprotective effect of the inclusion complex of  $\beta$ -cyclodextrin ( $\beta$ -CD) with the *bacuri* seeds hexanic extract (BSHE). In the characterization of the inclusion complex, an apparent stability constant ( $K_c$ ) of 416 mol/L was obtained in the solubility study; the BSHE: $\beta$ -CD m/m (g) complexation ratios at 1:9, 2:8, and 3:7 were 5.51%, 21.46%, and 20.11%, respectively. The formation of the BSHE: $\beta$ -CD inclusion complex was observed by FTIR technique, indicating the disappearance of bands characteristic of BSHE (2960  $\text{cm}^{-1}$  and 1755  $\text{cm}^{-1}$ ) when in the complex, compared to the spectra of pure BSHE or in physical mixture with  $\beta$ -CD, and by X-ray diffraction, which indicated a loss of crystallinity, typical signals of pure  $\beta$ -CD, and presentation of intense amorphization, characteristic of BSHE, incorporated in the  $\beta$ -CD pockets. In the evaluation of gastroprotective activity, through absolute ethanol-induced gastric lesions in mice, both BSHE and BSHE: $\beta$ -CD reduced gastric lesions, with 100 mg/kg dose of the complex having the greatest gastroprotective effect. BSHE: $\beta$ -CD was also able to reduce gastric lesions from ischemia and reperfusion, with the 50 mg/kg dose being the most effective. BSHE: $\beta$ -CD, also at this dose, reduced the MDA levels of the gastric mucosa, indicating a possible antioxidant activity in its gastroprotective effect. Thus, it was concluded that inclusion complex formation between  $\beta$ -CD and BSHE is possible, and that this formulation enhanced the gastric protective activity.

**Keywords:** *Platonia insignis* Mart; *bacuri*;  $\beta$ -cyclodextrin; ulcer; gastroprotection

## 1. Introduction

Natural products have been used as the main source of compounds for medicines, cosmetics, and food, being an important resource for technological development and

health maintenance [1–3]. Environmental, ecological, food resources, and health benefits are strictly linked under biodiversity perspectives: studies on the taxonomy of plants, increasing species variety, tracking species' biochemistry, intra-species biodiversity, or environmental influences and how these affect food quality and health advantages have become key issues [4]. Brazilian biodiversity represents a promising source for research on new active pharmacological compounds [1,5,6]. Despite Brazil being responsible for up to 20% of the living species known in the world, part of the Brazilian biological and chemical biodiversity remains unexplored [1].

Among the plant species native to Brazil, *Platonia insignis* Mart. (Clusiaceae), popularly known as *bacuri*, has been the subject of many studies. Studies have revealed that *bacuri* seeds have the following constituents: unsaturated fatty acids (oleic, stearic, and linoleic), diterpenes, and prenylated benzophenones, such as garcinielliptone (about 10–12% of the fatty extracts from *bacuri* seeds), diterpenes, alcohols, and long-chain hydrocarbons [7–9]. Pharmacological investigations of the extract of the seeds of *P. insignis* fruits report some activities, such as antioxidant [10,11], leishmanicidal [12], and anticonvulsant [13]. In addition, the decoction of fruit seeds is popularly used to treat diarrhea [14].

The gastric mucosa is often exposed to different harmful agents, endogenous (hydrochloric acid and pepsin) or exogenous (*Helicobacter pylori*, smoking, alcohol intake, use of NSAIDs, stress) that can trigger gastric ulcers and even tumors [15–18]. Peptide ulcers, for example, have some treatment models that can promote the healing of mucosal damage [18]. The antioxidant activity already proven for the extract of *bacuri* seeds may be important for the gastroprotective action of this vegetable derivative since free radicals can cause the appearance of ulcers and inflammatory processes in the gastrointestinal tract [19–23]. Several antioxidant compounds control the production of free radicals, which may have an endogenous origin or come from the diet and other sources (e.g., ascorbic acid,  $\beta$ -carotene, vitamin E, unsaturated fatty acids, and selenium) [19–22,24–27]. Antioxidants have the ability to stabilize or even deactivate such radicals before biological targets in cells are reached [28]. In general, the more hydroxyl substitutions, the stronger the antioxidant and prooxidant activities [29,30].

Cyclodextrins are organic molecules with a hydrophobic internal cavity and, therefore, capable of forming inclusion complexes with a wide variety of organic molecules, which can affect the physicochemical properties of the target molecule, such as antioxidant activity, water solubility, and stability [30,31]. Encapsulation can also increase dissolution rate, membrane permeability and bioavailability, mask flavor and increase product shelf life, providing protection against degradation of light or heat [32–35] also in the perspective of nanopharmaceutical and nanonutraceutical area, interesting in both pharmaceutical and food industries by possibility to control their properties using different types of raw materials [36–38].

Therefore, the present paper proposed the production and characterization of an inclusion complex  $\beta$ -cyclodextrin and hexanic extract of *bacuri* seeds and the evaluation of its gastroprotective effect in a gastric ulcer model.

## 2. Material and Methods

### 2.1. Drugs and Reagents

Garcinielliptone was isolated by silica gel column chromatography of the hexanic extract of the seeds of *P. insignis* Mart. and identified by hydrogen and carbon nuclear magnetic resonance and mass spectrometry [9,39]. For the extraction of raw materials, hexane (Labsynth, Diadema, SP, Brazil) was used, and in the preparation of the analysis solutions, methanol and absolute ethanol (Labsynth, Diadema, SP, Brazil). Commercially purchased were:  $\beta$ -cyclodextrin (Sigma-Aldrich, St. Louis, MO, USA), carbenoxolone, N-acetylcysteine (Eurofarma, Itapevi, SP, Brazil), Tween 80 (Sigma-Aldrich, St. Louis, MO, USA), sodium thiopental (Cristália, Itapira, SP, Brazil), 10% ketamine chloridate (Syntec), 2.0% chloridate xylasin (Syntec, Santana de Parnaíba, SP, Brazil), acetic acid (Labsynth,

Diadema, SP, Brazil), and thiobarbituric acid (TBA) and sodium dodecyl sulfate (SDS) from Sigma-Aldrich, St. Louis, MO, USA.

## 2.2. Extract Preparation and Procedures for Production and Characterization of a $\beta$ -Cyclodextrin Inclusion Complex with *Platonia Insignis* Seed Extract

### 2.2.1. Hexane Extract from *Platonia Insignis* Seeds

The *bacuri* seed was obtained at the Piauí Supply Center—CEAPI, and a desiccant was deposited at the Herbarium Graziella Barroso of the Federal University of Piauí, Brazil (under number: ICNTEPB27164). The seeds of the fruits were dried and powdered, following by extraction with hexane in Soxhlet for 8 h. The evaporation of the solvent was followed by a total extraction yield of 42.98% (Figure 1). The chromatographic profile of the *bacuri* seed hexane extract (BSHE) was obtained by high-resolution gas chromatography coupled to a mass spectrometer (HRCG/MS), using an Agilent chromatograph with a DB5 capillary column (J&W) (30 m  $\times$  0.25 mm  $\times$  0.25 m) in split mode (10:1). The chemical constituents were identified by the characteristic fragmentation and by comparison of the mass spectra obtained with the records of the NIST 2.0 computational library.

### 2.2.2. Phase Solubility Studies

The investigation of phase solubility was conducted according to Higuchi and Connors (1965) [40], in triplicate, adding the excess extract to test tubes containing aqueous solutions of  $\beta$ -cyclodextrin (Figure 1), in increasing concentrations (0–10 mmol/L). The solutions were heated to 50 °C for 10 min to solubilize the extract. The samples were kept in a water bath at 37 °C, under agitation, for two days. After the suspension reached equilibrium, aliquots were removed, filtered through filter paper, and diluted in methanol.

To carry out the quantification of the BSHE in the tests, a stock solution of this substance at a concentration of 0.2 g/L in methanol was scanned, from which a series of dilutions was prepared to obtain concentrations from 1 to 35 mg/L, with absorbance measurements at a wavelength of 280 nm. Equation (1) was used to calculate the apparent stability constant ( $K_s$ ) of the BSHE: $\beta$ -CD inclusion complexes from the slope of the phase solubility diagram and the solubility of BSHE in the absence of CD ( $S_0$ ).

$$K_s = \frac{\text{slope}}{S_0 (1 - \text{slope})} \quad (1)$$

### 2.2.3. Production of BSHE: $\beta$ -CD Inclusion Complexes

The inclusion complexes between the hexanic extract and  $\beta$ -CD were prepared by two methodologies [41] (Figure 1). In the first method, the mass refers to the extract being dissolved in 20 mL of ethanol, under heating and continuous agitation, and the mass referring to  $\beta$ -CD was dissolved in 250 mL of an ethanol:water mixture (1:4), under heating and agitation. The two solutions remained under stirring and heating at 70 °C for 35 to 40 min. Complexes were prepared in 1:9 proportions, 2:8; 3:7 BSHE: $\beta$ -CD m/m (g). The solution was injected into the bench-top spray dryer, BUCHI B-290, with an inlet pressure of 0.9 Bar, with a sample flow of 7 mL/min, inlet temperature of 105 °C, outlet temperature of 62 °C, and sample temperature of 60 °C. The other methodology used was that of BSHE: $\beta$ -CD by physical mixing, where the referent mass of the extract was mixed with the referent mass of  $\beta$ -cyclodextrin using grade and pistil.

### 2.2.4. Determination of Garcinielliptone FC by UV-Vis in BSHE and BSHE: $\beta$ -CD Inclusion Complexes

The garcinielliptone FC analytical curve was prepared using concentrations from 5 to 40 mg/L, for which absorbance measurements were read at a wavelength ( $\lambda$  max) of 280 nm, using a Varian Cary 300 double-beam spectrophotometer UV/Vis [42]. The reading wavelength was identified by scanning the garcinielliptone in methanol in the range of 200 to 400 nm. The analysis of the hexane extract by high-performance gas chromatography (HPGC-MS) allowed verifying 16 chemical constituents in the total ion

chromatogram. The hexane extract has a composition rich in fatty acid esters, obtaining the following constituents with the respective contents (Table 1). It should be noted that peak 12 represents the major constituent of the extract, which is a prenylated benzophenone.

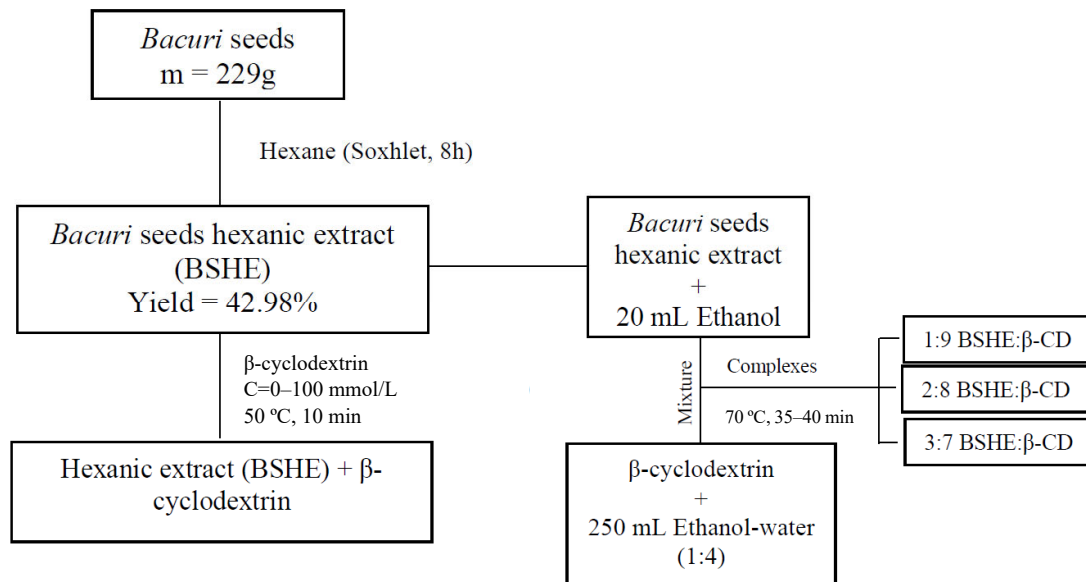


**Figure 1.** Graphical scheme of extract preparation (BSHE) and procedures for the production of a  $\beta$ -cyclodextrin inclusion complex with *Platonia insignis* seed extract.

**Table 1.** Chemical constituents (%) hexanic extract of the seeds of *P. insignis* Mart.

Peak	Constituents	Tr (min)	Area (%)
1	Methyl ester of palmitoleic acid C16:1 cis 9	19.131	0.44
2	Palmitic acid methyl ester C16:0	19.934	4.66
3	Palmitic acid ethyl ester C16:0	22.033	0.42
4	Linolenic acid methyl ester C18:3 cis, cis, cis 9,12,15	24.596	0.13
5	Linoleic acid methyl ester C18:2 cis, cis 9,12	24.747	0.17
6	Oleic acid methyl ester C18:1 cis 9	24.93	3.57
8	Stearic acid methyl ester C18:0	25.647	0.49
9	Gadoleic acid methyl ester C20:1 cis 9	26.599	0.18
10	Squalene	39.48	0.52
11	GFC (garcinielliptone FC)	41.037	0.50
12	Prenylated benzophenone ( $\gamma$ -mangostine)	43.754	77.35
13	Campesterol	46.122	0.74
14	Stigmasterol	46.506	1.14
15	Sitosterol	47.447	1.06
16	Lanosterol	47.93	3.45

Through the analytical curve of garcinielliptone FC produced, it was determined that the concentration of garcinielliptone in the hexane extract was  $7.71\% \pm 0.47$ , which has anti-inflammatory activity [13,43,44].

To determine the garcinielliptone content in the complexes, the garcinielliptone analytical curve was used, and the non-complexed extract was removed from the  $\beta$ -cyclodextrin molecules by washing the complexes formed with hexane. For this, 8 mL of hexane was added and dissolved for a few seconds in the ultrasound; the supernatant liquid was slowly aspirated with a dropper, performing this procedure in triplicate for each complex until only complexed extract was left. Then, the complexes were stored in a desiccator until drying and UV/Vis analysis. The washed complexes removed from the desiccator were dissolved in methanol, and the volume was made up to 10 mL, being analyzed at 280 nm in triplicate.

### 2.2.5. Characterization of BSHE: $\beta$ -CD Inclusion Complexes

The FT-IR spectra of samples were recorded using an FT-IR spectrometer (Varian 660-IR) equipped with a diamond crystal cell for attenuated total reflection (ATR). The spectra were obtained (32 scans per sample or background) in the range of 400–4000  $\text{cm}^{-1}$  range with a nominal resolution of 4  $\text{cm}^{-1}$  at room temperature. The air as a background spectrum was used to adjust the spectra. A lyophilized/powder sample was applied to the ATR crystal surface for the measurements. The ATR crystal was meticulously cleaned using wet cellulose tissue before being dried with a flow of nitrogen gas. To make sure that no residue from the prior sample was left on the cleaned crystal, it was spectrally inspected. Each sample spectrum was captured five times in order to assess its reproducibility and perform statistical analysis. A Shimadzu model XRD-6000 X-ray diffractometer with Cu radiation was used to conduct the XRD experiments. At a scan rate of  $2^\circ/\text{min}$ , the samples were scanned from  $2\theta = 10\text{--}55^\circ$ . To maintain a flat sample plane, the powder sample was spread out on a glass plate, and measurements were taken.

## 2.3. In Vivo Study by Animal Model: Performance as Gastroprotective System

### 2.3.1. Animal Models

Mice (*Mus musculus*, Swiss variety) were used, weighing between 25 and 30 g, and rats (*Ratus norvegicus*, Wistar lineage), weighing 180 to 220 g, were supplied by the Animal Facility from Research Center for Medicinal Plants from the University Federal of Piauí (Teresina, Brazil). The animals were maintained in standard cages at a controlled temperature ( $24 \pm 1^\circ\text{C}$ ) and a 12 h light/dark cycle, with free access to water and food. They fasted for a period of 18 h and were acclimatized to the test environment for 2 h before each experiment. In all experiments, the animals were kept in raised cages with a wide mesh floor to avoid coprophagy. After the experimental procedures, the animals were euthanized with an overdose of sodium thiopental (100 mg/kg, i.p.). The experimental protocols were approved by the Ethics Committee on the Use of Animals of Universidade Federal do Piauí (Teresina, Brazil) under approbation no. CEEA-PI 008/12.

### 2.3.2. Ethanol-Induced Gastric Ulcer

After an 18 h fasting period, mice were randomly divided into groups of six animals. Acute gastric lesions were induced by intragastric administration of absolute ethanol in a volume of 0.2 mL per animal [45]. According to the division of the animal groups, 1 h before the application of the ulcerogenic agent, it was administered orally: BSHE (25, 50, and 100 mg/kg), BSHE: $\beta$ CD (25, 50, and 100 mg/kg), saline (negative control) or carbenoxolone (100 mg/kg). After 30 min, The stomach was taken out and opened along the point of greatest curvature after the animals were euthanized. The stomachs were scanned, and the percentage (%) of the ulcerated region in relation to the overall stomach area was determined using the Image J software (Figure 2) [46]. A glandular part of the stomach was used for malondialdehyde assay.

### 2.3.3. Gastric Lesions Induced by Ischemia and Reperfusion in Rats

Wistar rats ( $n = 6/\text{group}$ ) were treated orally with saline, N-acetylcysteine (200 mg/kg), BSHE (25; 50 and 100 mg/kg), or BSHE: $\beta$ -CD inclusion complexes (25, 50, and 100 mg/kg). After 30 min, the animals were anesthetized (ketamine 30 mg/kg and xylazine 0.3 mg/kg) by intraperitoneal injection (Figure 2). An incision was made in the abdomen, and after the location of the celiac artery, the animals were subjected to 30 min of ischemia induced by the occlusion of the artery by a microvascular clamp and followed by reperfusion of 1 h according to the adapted method by Ueda and Okada [47]. Then, the animals were euthanized, and their stomachs were removed and prepared for analysis, as mentioned above.

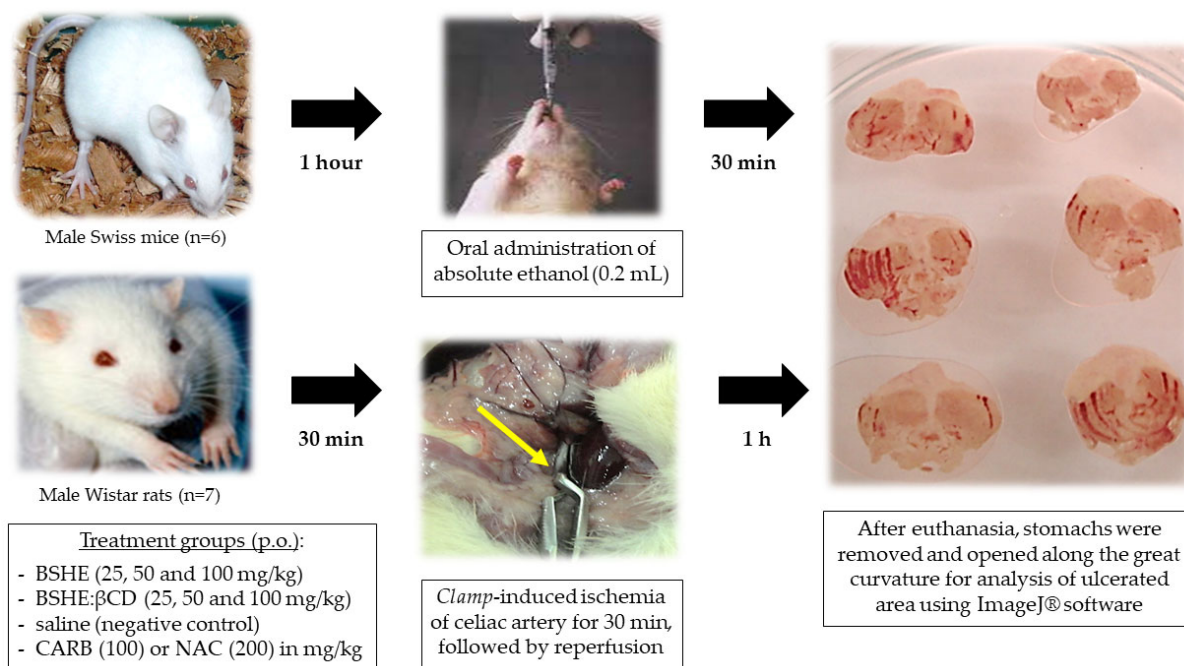


**Figure 2.** General scheme of ethanol and ischemia/reperfusion-induced gastric ulcers in rodents. Legend: CARB = carbenoxolone; NAC = N-acetylcysteine.

#### 2.3.4. Dosage of Malonaldehyde (MDA)

A total of 100 mg of the glandular part of the stomach was weighed and cut into small pieces and stored at  $-70^{\circ}\text{C}$ . Then, 1 mL of phosphate buffer was added and homogenized in a tissue crusher. It was centrifuged at  $10,000 \times g$  rpm at  $4^{\circ}\text{C}$  for 5 min. A total of 300  $\mu\text{L}$  of the supernatant was pipetted, and a mixture of 350  $\mu\text{L}$  of acetic acid (pH 3.5) and 600  $\mu\text{L}$  of diluted thiobarbituric acid (TBA) at 0.5% was added. The tubes were shaken every 15 min while they were held in a water bath at  $85^{\circ}\text{C}$  for 1 h, followed by a freezing bath for 15 min. Afterward, each tube received 50  $\mu\text{L}$  of 8.1% sodium dodecyl sulfate (SDS). The tubes were then centrifuged for 15 min at  $12,000 \times g$  rpm and  $25^{\circ}\text{C}$ . After removing the supernatant, the spectrophotometer was read at 510, 532, and 560 nm [48].

#### 2.4. Statistical Analysis

The results were presented as mean  $\pm$  S.E.M. (standard error of the mean). The data obtained were evaluated using analysis of variance (ANOVA) followed by the Tukey test using GraphPad Prism version 5.0. The differences were considered significant when values of  $p < 0.05$ .

### 3. Results and Discussion

#### 3.1. Characterization of the BSHE:β-CD Inclusion Complexes

Cyclodextrins (CDs) are water-soluble cyclic oligomers derived from starch used to improve the solubility, stability, and bioavailability of drugs [49–52]. In addition, some studies have reported that the formation of the inclusion complex can prolong and increase the duration and intensity of medications [49–53]. Cyclodextrins can be found in more than 35 commercially available drugs, including pills, parenteral solutions, eye drops, ointments, and suppositories [54–57].

The formation of the inclusion complex is facilitated by the removal of water molecules from the inside of the DC cavity, partially hydrophobic, and their replacement by nonpolar molecules spontaneously, being, therefore, an energetically viable process [49]. This process is facilitated by the action of several forces of interactions, such as the formation of hydrogen bonds, van der Waals interactions, the very change in the surface tension of the medium,

and the reduction of the tension of the cyclodextrin ring, which, combined, strongly influence the formation of the inclusion complex [53,55–57].

Figure 3 corresponds to the concentration of BSHE versus the concentration of cyclodextrin. In order to calculate the stability constant ( $K_c$ ) and the stoichiometry of the complex formation from the intrinsic solubility of the substrate ( $S_0$ ) and the slope of the straight line resulting from the solubility diagram, the complexation study allows for the analysis of the solubility results of the guest molecule in solutions with increasing concentrations of CDs [55,56,58–60].

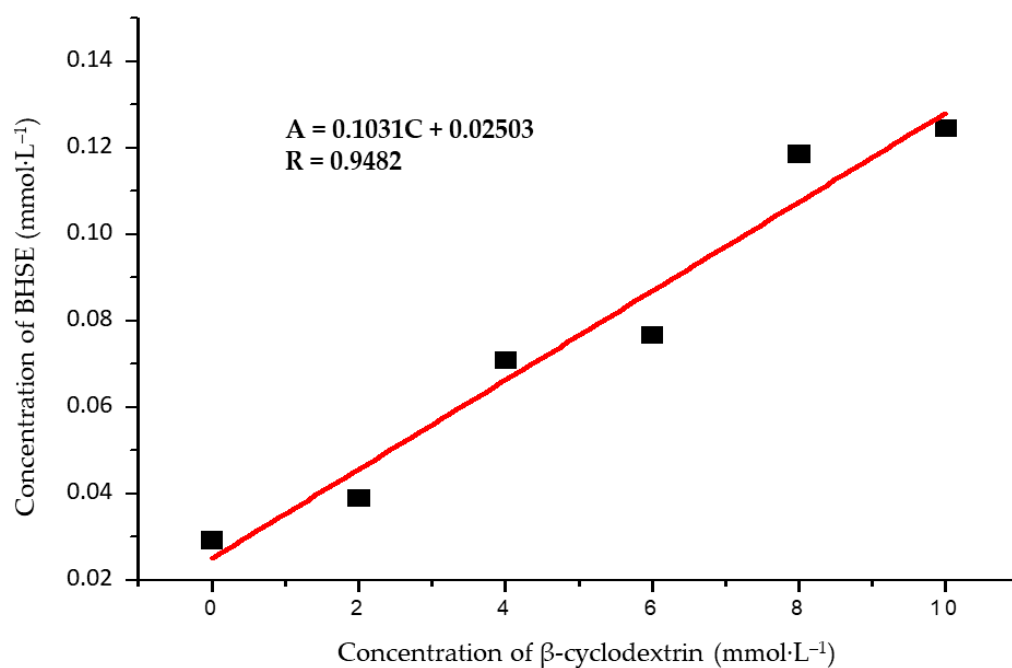


**Figure 3.** Solubility diagram of the BSHE:β-CD inclusion complexes.

The average molar mass of the BSHE, necessary for the realization of the diagram, was obtained through the analysis of the chemical constituents of the hexanic extract and their respective contents, obtained through the total ion chromatogram of the fraction of this extract, as shown in Table 1. The diagram obtained from β-CD is of the increasing linear type because its solubility increases in direct proportion to the concentration of the complexing agent. From the diagram, the angular coefficient was obtained, with a result of less than 1 (0.1031), indicating the stoichiometry of the 1:1 complex [61–63].

From the straight-line equation obtained from the β-CD solubility diagram, the stability constant ( $K_c$ ) was calculated based on the equations created by adapting Higuchi and Connors (1965), which assesses the mechanism by which the solution containing cyclodextrin (CD) and drug (F), forms the complex (CD.F), and complexation efficiency ( $E_c$ ) [62–65], described below (Equations (2)–(4)):

$$K_{C1:1} = \frac{\text{Angular coefficient}}{S_0 (1 - \text{Angular coefficient})} \quad (2)$$

$$E_c = \frac{\text{Angular coefficient}}{(1 - \text{Angular coefficient})} \quad (3)$$



The higher the ( $K_c$ ) value obtained, the easier it is to form an inclusion complex. In the inclusion complex formed between the hexanic extract of bacuri seeds and the β-CD molecule, a constant value ( $K_c$ ) of 416 mol/L was obtained. In pharmaceutical terms, it is desirable to use formation complexes whose constant is between 100 and 1000 M<sup>-1</sup>.

Drugs having a lower formation constant form unstable complexes, while those with high formation constants are too stable to release the drug into the body [66]. Therefore, Figure 1 shows that EHSB complexation is feasible and can improve the solubility of the system in view of the characteristics of cyclodextrin. For the aspect ratio 1:9, 2:8, and 3:7 of EHSB: $\beta$ -CD ( $w/w$ ), complexation yields were, respectively, 5.51%, 21.46%, and 20.11%. Possessing a better complexation ratio, the BSHE: $\beta$ -CD 3:7 formulation was chosen in the gastroprotection protocols for its higher content of the marker garcinielliptone and better antioxidant activity [67].

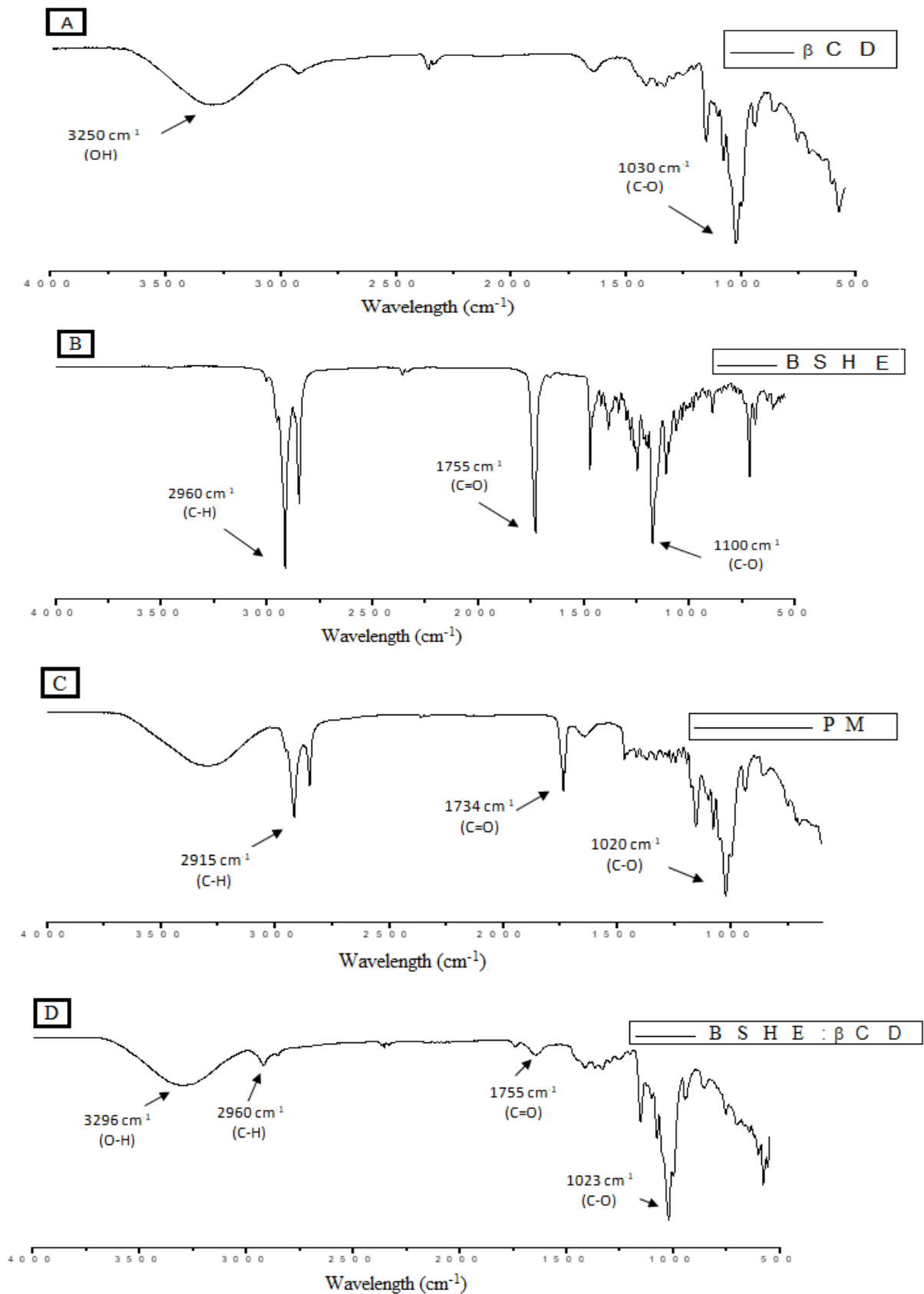
This could be related to the fact that during the complexation process, not all molecules are able to penetrate the cyclodextrin cavity, either due to their size, their weak affinity, or even the excessive amount of drug compared to the amount of cyclodextrins for complexation [62,63,65,66]. Therefore, in a complexation process, there will be free drug, complex drug, and free cyclodextrin, in balance [58,59,62,63]. The challenges for complexation processes include nonpolar molecules (or functional groups of molecules) whose dimensions are smaller than those of the cyclodextrin cavity that can be included in that cavity [68,69]. The dynamic balance between free drug molecules and complexed drug molecules is quantitatively described by the stability or association constant, where there is the existence of complex drug, free drug, and free CD [70–72].

Figure 4 shows the FT-IR spectra of the BSHE: $\beta$ -CD inclusion complexes. By comparing the infrared spectra of the pure drug, cyclodextrin, and the solid complexes obtained by various production methods [59,69–73], one may assess the formation of inclusion complexes in the solid phase. The vibrational spectrum of the various functional groups of the complexed or free drug molecules is used to detect substantial changes in the shape and location of the absorption bands, hence verifying interactions at the molecular level [74–77]. FT-IR spectroscopy can be viewed as a “fingerprint analytical technique” that allows the structural identification of compounds, considering that two chemical structures will not provide the same FT-IR spectrum [78]. By highlighting their molecular vibrations, or the stretching, bending, and torsion of the chemical bonds, in specific infrared areas, FT-IR provides typical characteristics of chemical or biochemical components in the samples.

Even though cyclodextrin and BSHE’s interactions in the inclusion complex are not particularly strong, since they are non-covalent electrostatic bonds (Van der Waals, hydrophobic interactions, hydrogen bonds) [79–82], deviations and changes in the intensity of several bands are observed when we compare the isolated spectra of BSHE and  $\beta$ -cyclodextrin molecule. In the spectrum of  $\beta$ -cyclodextrin (Figure 4A), a broadband of medium intensity in  $3250\text{ cm}^{-1}$  is observed, attributed to the stretching of the O-H bonds, and a strong band in  $1030\text{ cm}^{-1}$ , attributed to the stretching of the simple C-O bond. The BSHE’s infrared spectrum shows a marked absorption in  $2960\text{ cm}^{-1}$  as main bands, related to the asymmetric stretch C-H of alkanes; in  $1755\text{ cm}^{-1}$ , it also has a strong band related to the stretching of the C=O bond of esters and/or ketone and in  $1100\text{ cm}^{-1}$  plus a strong absorption band, related to the simple CO bond stretching of esters (Figure 4B).

Figure 4C shows an overlap of the patterns of the physical mixture BSHE: $\beta$ -CD. The characteristic bands of BSHE and  $\beta$ -CD ( $2915\text{ cm}^{-1}$ ,  $1734\text{ cm}^{-1}$ , and  $1020\text{ cm}^{-1}$ ) were identified, demonstrating that there was a weak interaction between the extract and  $\beta$ -CD. In the formation of the inclusion complex BSHE: $\beta$ -CD (Figure 4D), it shows that the bands in  $2960\text{ cm}^{-1}$  and in  $1755\text{ cm}^{-1}$  decreased a lot in intensity, reaching almost the disappearance. These phenomena are associated with the insertion of a molecule into the  $\beta$ -CD cavity, which causes a conformational restriction, reducing the free movement of encapsulated molecules and contributing to the reduction of the intensity of their signals. The band  $1030\text{ cm}^{-1}$  shifted to  $1023\text{ cm}^{-1}$  and increased in intensity, indicating a convolution of peaks.

The spectra of inclusion complexes in different proportions of BSHE: $\beta$ -CD were also analyzed (Supplementary 1). The three proportions of 2:8, 3:7, and 1:9 m/m (g) of BSHE: $\beta$ -CD demonstrate that there was a suitable complexation between the molecule BSHE and  $\beta$ -CD, as there was an intense decrease in the characteristic peaks of BSHE, without significant differences between the complexes.



**Figure 4.** Infrared spectrum of samples containing BSHE and  $\beta$ -CD. (A)  $\beta$ -cyclodextrin molecule, (B) bacuri seed hexane extract (BSHE), (C) physical mixture between BSHE: $\beta$ -CD, and (D) BSHE: $\beta$ -CD inclusion complexes.

The formation of the inclusion complex was also verified by the P-XRD spectrum [83,84]. X-ray diffraction (XRD) is one of the best techniques for the characterization of inclusion complexes due to its simplicity and speed because it allows a morphological study of the substances and their structures and/or crystalline fractions [85–89]. The guest molecules replace the enthalpy-rich water molecules from the inner cavity during the development of an inclusion complex. This results in modifications to the crystal lattice, which alter the inclusion complex's XRD pattern [90]. When compared to the pattern of the complexes, they exhibit stronger crystallinity. The diffraction pattern of a physical mixture often involves the overlapping of the patterns of the guest molecule and the  $\beta$ -CD with peaks of smaller intensity [91]. When the formation of inclusion complexes occurs, changes in the characteristic peaks of the host molecule can form new peaks, which indicate a new solid phase, which corresponds to the drug- $\beta$ -CD complex [92].

The analysis of the  $\beta$ -CD molecule by XRD (Figure 5) shows that there is the formation of several diffraction peaks, presenting itself as a high crystalline compound. The  $\beta$ -CD diffractogram showed characteristic peaks at  $2\theta = 9.30^\circ, 10.72^\circ, 12.88^\circ, 15.50^\circ, 17.20^\circ, 22.81^\circ, 27.23^\circ,$  and  $32.01^\circ$ . The BSHE has an amorphous characteristic, with some characteristic peaks at  $2\theta = 19.24^\circ, 22.70^\circ,$  and  $23.22^\circ$ . The physical mixture BSHE: $\beta$ -CD shows a diffraction pattern similar to that of  $\beta$ -CD, but with some changes in the baseline, either due to the decrease and/or displacement of peaks very characteristic of  $\beta$ -CD at  $2\theta = 9.19^\circ, 10.71^\circ, 12.70^\circ, 15.50^\circ,$  and  $17.21^\circ$ . This indicates the presence of BSHE (by decreasing the peaks) and a small interaction between BSHE and  $\beta$ -CD.

In the inclusion complex BSHE: $\beta$ -CD, alterations in the diffraction patterns referring to  $\beta$ -CD and BSHE alone were observed. The number and intensity of the signals were reduced, characterizing loss of crystallinity and presenting intense amorphization with the observation of only two broad bands of low intensity, at  $2\theta = 12.84^\circ$  and  $18.49^\circ$ . Obtaining a diffractogram that resembles an amorphous material, that is, one without clearly defined fine peaks may be a sign that complexation has occurred [93].

### 3.2. Gastroprotective effect of BSHE: $\beta$ -CD Inclusion Complexes

The loss of crucial defense mechanisms, such as a reduction in the activity of antioxidant enzymes, the destruction of the gastric mucus barrier, the production of reactive oxygen species (ROSs), which causes oxidative stress, and the activation of the innate immune system, are characteristics of the gastric lesion caused by ethanol [94]. In the present study, gastric ulcers were induced in mice to assess the gastroprotective effect of BSHE: $\beta$ -CD inclusion complexes (Figure 6). The administration of oral ethanol (96%, 0.2 mL/animal) to mice treated with saline (negative control) caused severe damage to the gastric mucosa, clearly producing the expected characteristic zone of necrotizing lesions of the mucosa, generally parallel along the stomach body axis (Figure 6A). As marked in Figure 6A, the lesions can be seen by the white arrows that point to formed stretches. BSHE (Figure 6B), BSHE: $\beta$ -CD (Figure 6C), and carbenoxolone (Figure 6D) decreased the effect of stretch marks, suggesting the gastroprotective effect.

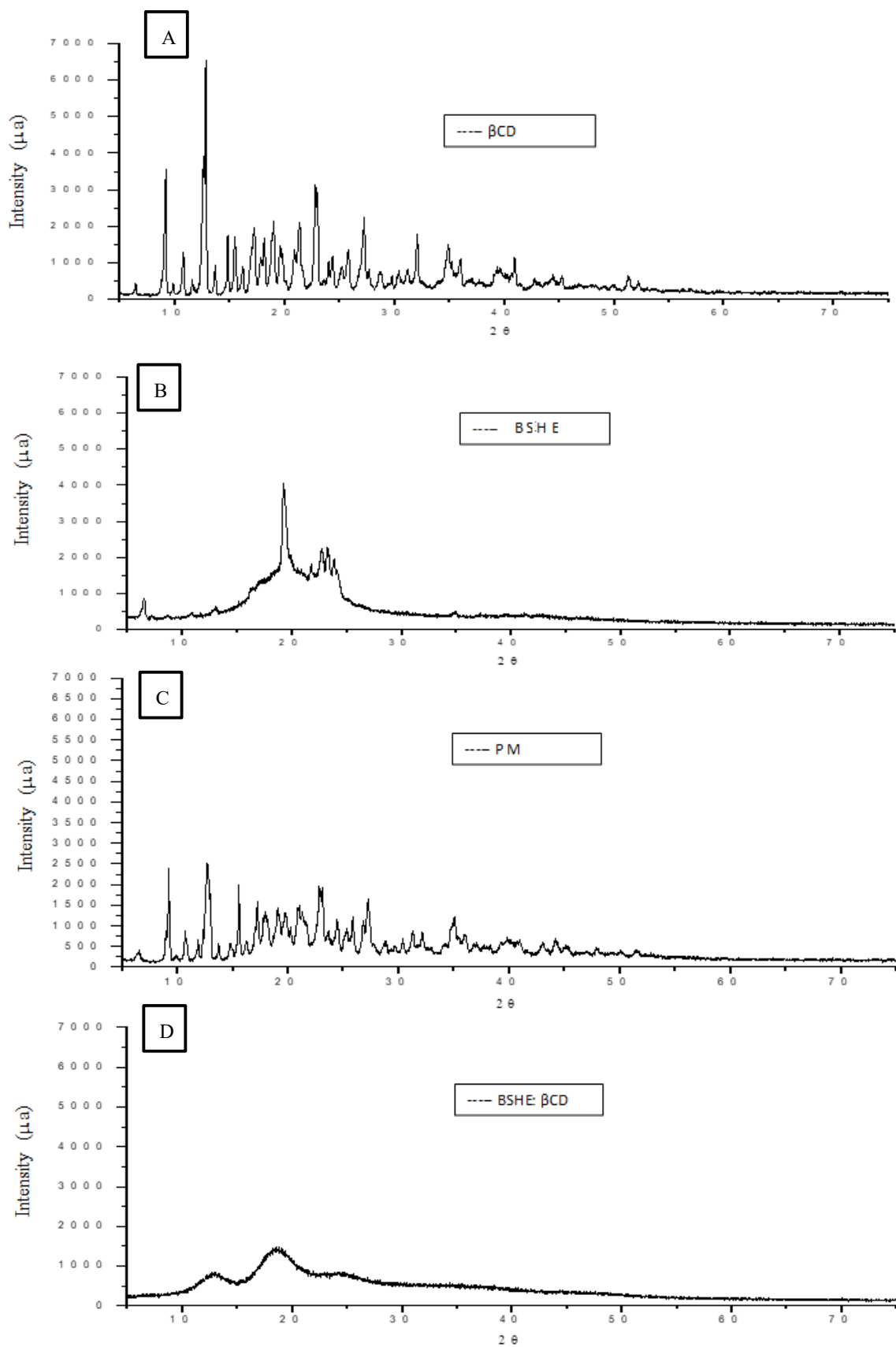


**Figure 5.** X-ray diffraction (XRD) of samples containing BSHE and  $\beta$ -CD. (A)  $\beta$ -cyclodextrin molecule, (B) bacuri seed hexane extract (BSHE), (C) physical mixture between BSHE: $\beta$ -CD, and (D) BSHE: $\beta$ -CD inclusion complexes.

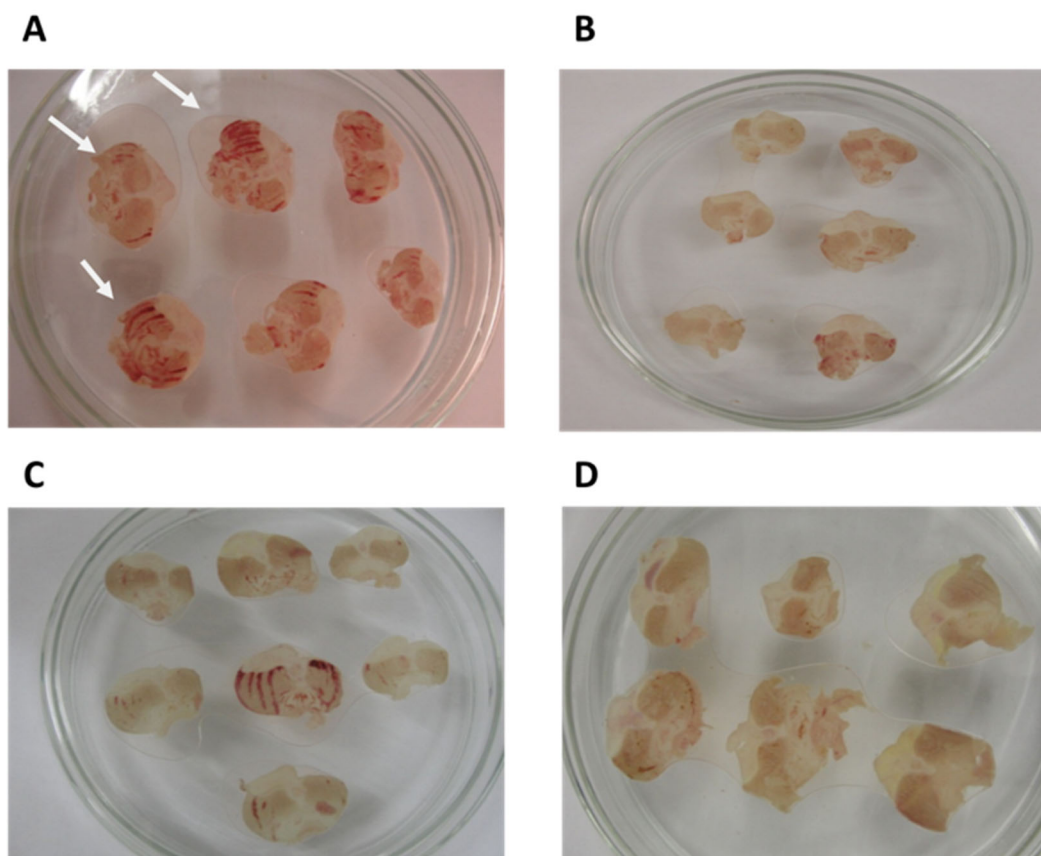


**Figure 6.** Injury area of the gastric mucosa of the stomachs in mice. (A) Negative control treated with saline, (B) BSHE administered in the proportion of 100 mg/kg, (C) BSHE:β-CD inclusion complexes in the proportion of 100 mg/kg, (D) positive control: carbenoxolone (100 mg/kg). (The white arrows signal the stretches).

Figure 7 shows the analysis of gastroprotective activity BSHE:β-CD inclusion complexes in gastric lesions induced by absolute ethanol in mice. Through the lesion area analysis, it can be confirmed that both BSHE and BSHE:β-CD show gastroprotective activity in this assay (Figure 7). The gastric lesion observed in the control group (saline) was  $26.70 \text{ mm}^2 (\pm 2.56)$  of the mucosa area. When compared with the negative control, the animals treated with BSHE and BSHE:β-CD inclusion complex showed a significant reduction in the area of gastric lesions. BSHE at doses of 25 and 50 mg/kg reduced lesion area to  $10.50 \text{ mm}^2 \pm 2.48$  (60.70%) and  $8.72 \text{ mm}^2 \pm 1.68$  (67.40%), respectively; for BSHE:β-CD, the same doses reduced it to  $8.53 \text{ mm}^2 \pm 1.55$  (68.10%) and  $9.6 \text{ mm}^2 \pm 1.10$  (64.10%), respectively, showing significant lesion area reduction compared with the negative control, but without significance between them.

The BSHE:β-CD inclusion complex at a dose of 100 mg/kg had the same effect as carbenoxolone and was more effective than BSHE (Figure 7). Animals treated with carbenoxolone (positive control) at a dose of 100 mg/kg had a decrease in ulcerative lesions of  $2.34 \text{ mm}^2$ , promoting 91.20% inhibition of the ulcerative lesion. The animals treated with BSHE:β-CD inclusion complexes at a dose of 100 mg/kg had a decrease in ulcerative lesions of around 89.5% (area equivalent to  $2.8 \text{ mm}^2$ ) when compared with carbenoxolone. These results justify the complexation to obtain better effects of a possible phyto-medication obtained from the extract of the seeds of *Platonia insignis* since BSHE:β-CD inclusion complexes in the proportion of 100 mg/kg proved to be more effective than the EHSB. It should be noted that the BSHE:β-CD inclusion complexes are in the proportion of 3:7 (BSHE:β-CD), that is, only 30% of the pure BSHE.

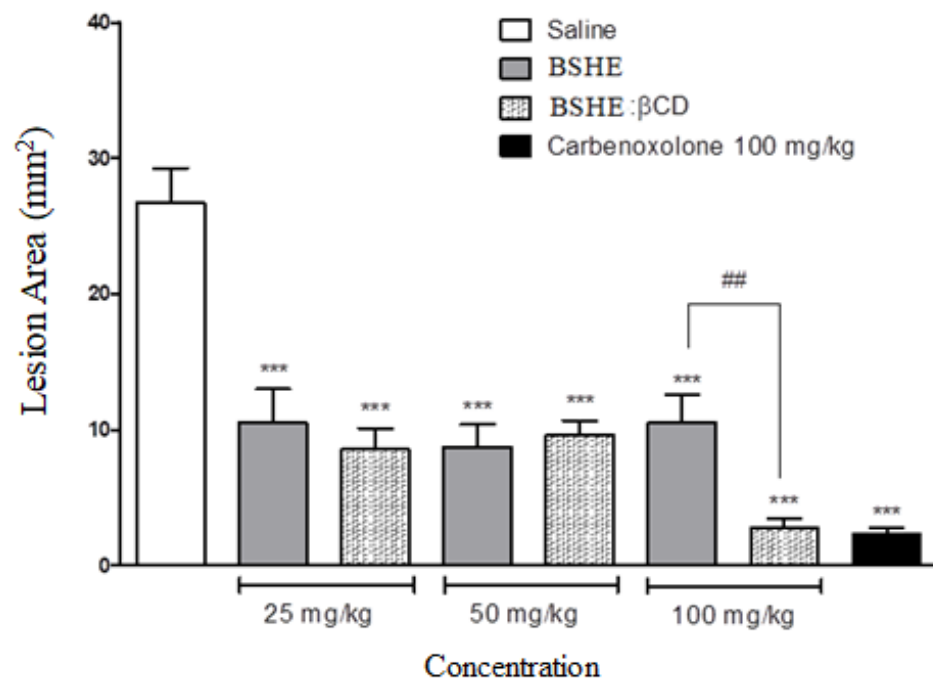


**Figure 7.** Analysis of gastroprotective activity BSHE:β-CD inclusion complexes in gastric lesions induced by absolute ethanol in mice. BSHE and BSHE:β-CD inclusion complexes were used at doses of 25, 50, and 100 mg/kg. For negative control, saline was used, and for positive control, carbenoxolone (100 mg/kg) was used. Data are expressed as mean ± E.P.M., \*\*\*  $p < 0.001$ , compared to control (ANOVA, followed by Tukey's test), ##  $p < 0.01$  comparing BSHE with BSHE:β-CD inclusion complexes.

The presence of terpenes and flavonoids in the BSHE may justify the inhibitory activity on gastric ulceration [95,96]. Phenolic compounds have an antiulcerogenic effect related to cytoprotective activity [97]. The *Platonia insignis* Mart. has a high content of flavonoids and sesquiterpenes [98–100].

Figure 8 shows the results of the protective effect in an ischemia and reperfusion (RI) ulcer model. The saline group presented  $10.34 \text{ mm}^2 \pm 1.05$  of gastric lesion area. The BSHE showed a significant decrease in gastric injuries areas at doses of 25, 50, and 100 mg/kg, which was of  $5.12 \text{ mm}^2 \pm 0.52$ ,  $3.76 \text{ mm}^2 \pm 0.85$ , and  $2.68 \text{ mm}^2 \pm 0.39$ , respectively, showing a gastroprotection percentage of 50.50%, 63.60%, and 74.10%, respectively, when compared to the negative control group. Furthermore, the BSHE:β-CD inclusion complex also showed a decrease in lesions area of  $3.97 \text{ mm}^2 \pm 0.82$ ,  $2.70 \text{ mm}^2 \pm 0.52$ , and  $2.48 \text{ mm}^2 \pm 0.41$  at concentrations of 25, 50, and 100 mg/kg, respectively, leading to a reduction percentage in 61.60%, 73.90%, and 76.10% when compared to saline group. The positive control (N-acetylcysteine) reduced the lesions by 79.40% (area equivalent to  $2.13 \text{ mm}^2$ ). These results demonstrate that the BSHE and BSHE:β-CD inclusion complex have excellent gastroprotective activity, with an inhibition statistically similar to the positive control, which is a derivative of the natural amino acid cysteine and acts as a precursor to the reducing agent glutathione, an endogenous molecule with a crucial role in the defense mechanism of toxic agents and gastric ulcers [101–104].

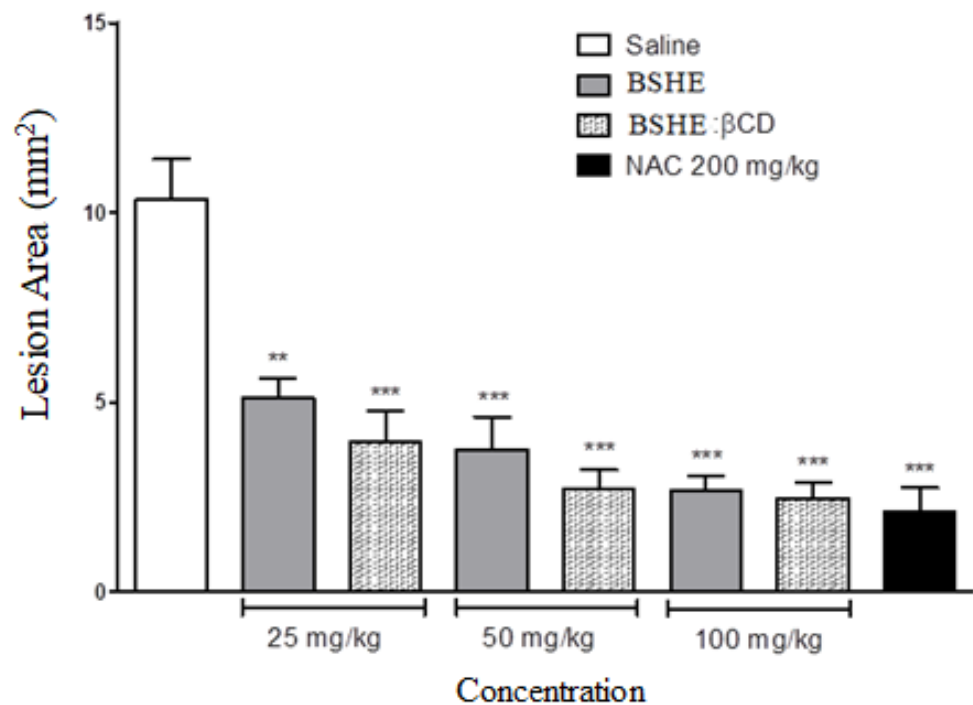


**Figure 8.** Analysis of gastroprotective activity BSHE:β-CD inclusion complexes in gastric lesions induced by I/R in rats. BSHE and BSHE:β-CD inclusion complexes were used at doses of 25, 50, and 100 mg/kg. For negative control, saline was used, and for positive control, N-acetylcysteine (200 mg/kg) was used. Data are expressed as mean ± E.P.M., \*\*  $p < 0.01$  and \*\*\*  $p < 0.001$ , compared to control (ANOVA, followed by Tukey's test).

The ischemia and reperfusion (IR) ulcer model is used to assess drug response in an ulcerogenesis process without the use of chemical agents, pathogens, or somatic stress, as in the ethanol, *H. pylori* and cold and containment models, isolating ulcerative factors related to free radicals formed by inflammatory and vascular processes [105–108]. The perfusion of the gastric mucosa is an essential factor in the ability of the mucosa to protect itself against injuries, and its defense is reduced in ischemic conditions, resulting in cell death and damage to the mucosa [109–113]. Ischemia is able to induce lesions in the gastric tissue; however, after reperfusion, there are the main damaging events that can increase by about three times in relation to those caused in the ischemia process [114]. The results of gastroprotection activity by I/R (Figure 8) suggest that the protection of the lesions may be related to the antioxidant activity of the bacuri extract.

Figure 9 shows the evaluation of malonaldehyde (MDA) production in gastric tissues. MDA is a biomarker of the damage caused by reactive oxygen and nitrogen species (EROs and ERNs) derived from the lipid peroxidation of cell membranes [115–118]. In the present study, a reduction in malonaldehyde levels after treatment with BSHE, BSHE:β-CD inclusion complexes, and carbenoxolone was observed. The chemical components of *Platonia insignis*, such as xanthenes and benzophenones, have antioxidant activity similar to the activities catalyzed by superoxide dismutase [99,100]. Thus, the results indicate that BSHE:β-CD inclusion complexes may carry this compound types, which has promising potential application for gastroprotection.

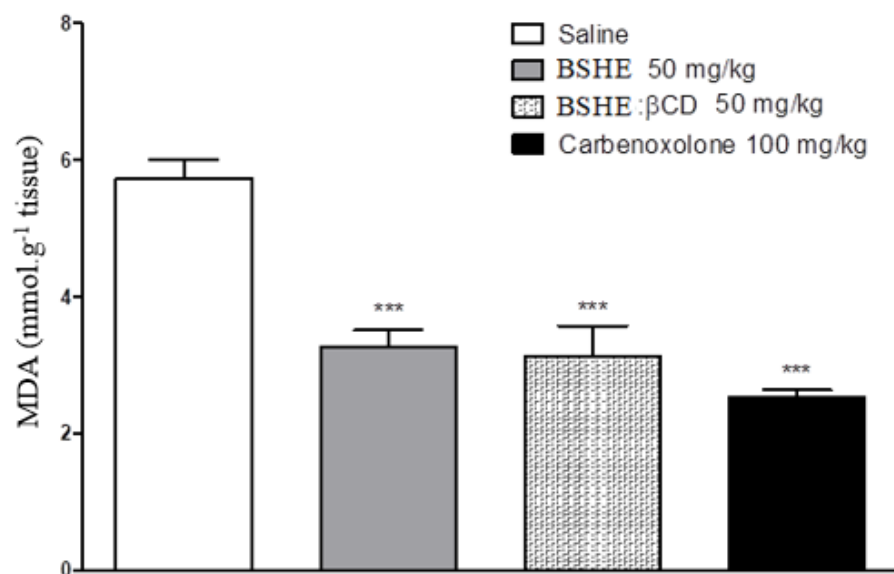


**Figure 9.** Detection of MDA in gastric tissue with gastric ulcer. BSHE, BSHE:β-CD inclusion complexes, and carbenoxolone (positive control) were used in concentrations of 50 mg/kg, 50 mg/kg, and 100 mg/kg, respectively. For negative control, saline was used. Data are expressed as mean ± E.P.M., \*\*\*  $p < 0.001$ , compared to control (ANOVA, followed by Tukey's test).

#### 4. Conclusions

In the context of plant resources as a promising source of natural products, the exploration of *Platonia insignis* features and the new formulation is here focused. The present study demonstrated success in the process of construction of the BSHE:β-CD inclusion complexes allied to the nanonutraceutical area. Moreover, this product was capable of preserving and enhancing the gastroprotective effect of BSHE against gastric lesion models once it reduces injured areas with less amount of this vegetal derivative inside the β-CD complexes. Furthermore, this study opens for the further development of nanoformulations using fruits byproducts as biomass, as achieved for seeds of *P. insignis* in this work. In this sense, toxicological studies are additionally recommended to ensure safety allied to a wide possibility of pharmacological and nutraceutical applications.

**Author Contributions:** Conceptualization, R.d.C.M.O., A.D., D.D.R.A. and A.M.d.G.L.C.; methodology, B.Q.A., M.d.S.R., J.S.d.C.-J., R.d.C.M.O., D.D.R.A. and A.M.d.G.L.C.; validation, A.G.C., B.Q.A., F.d.C.P.d.A. and H.d.B.F.; formal analysis, C.d.O.B., H.d.B.F., A.N.M. and J.S.d.C.-J.; investigation, J.L.N., Y.S.O.B., I.S.O., F.V.d.S., A.F.S.C.V. and M.d.S.R.; resources, R.d.C.M.O. and A.M.d.G.L.C.; data curation, D.D.R.A., M.L. and A.D.; writing—original draft preparation, J.L.N., Y.S.O.B., H.d.B.F. and A.N.M.; writing—review and editing, C.d.O.B., R.d.C.M.O., M.L., A.D., D.D.R.A. and A.M.d.G.L.C.; visualization, J.L.N.; supervision, A.M.d.G.L.C.; project administration, D.D.R.A.; funding acquisition, R.d.C.M.O. and A.M.d.G.L.C. All authors have read and agreed to the published version of the manuscript.

**Funding:** This research received no external funding.

**Institutional Review Board Statement:** The animal study protocol was approved by the Ethics Committee on the Use of Animals of Universidade Federal do Piauí (Teresina, Brazil) (CEEA-PI No. 008/12, approved on 16 May 2012).

**Informed Consent Statement:** Not applicable.

**Data Availability Statement:** Not applicable.

**Acknowledgments:** We are grateful to Coordination for the Improvement of Higher Education Personnel (CAPES, Brazil) and State Research Support Foundation of Piauí (FAPEPI, Brazil).

**Conflicts of Interest:** The authors declare no conflict of interest.

## References

1. Pilon, A.C.; Valli, M.; Dametto, A.C.; Pinto, M.E.F.; Freire, R.T.; Castro-Gamboa, I.; Andricopulo, A.D.; Bolzani, V.S. NuBBEDB: An updated database to uncover chemical and biological information from Brazilian biodiversity. *Sci. Rep.* **2017**, *7*, 7215. [[CrossRef](#)]
2. Ramadan, M.F.; Durazzo, A.; Lucarini, M. Advances in Research on Food Bioactive Molecules and Health. *Molecules* **2021**, *26*, 7678. [[CrossRef](#)]
3. Figueiredo, A.; Hugueney, P.; Durazzo, A. Recent Advances in Plant Metabolomics: From Metabolic Pathways to Health Impact. *Biology* **2022**, *11*, 238. [[CrossRef](#)]
4. Durazzo, A.; Lucarini, M. Environmental, Ecological and Food Resources in the Biodiversity Overview: Health Benefits. *Life* **2021**, *11*, 1228. [[CrossRef](#)] [[PubMed](#)]
5. Tabajara de Oliveira Martins, D.; Rodrigues, E.; Casu, L.; Benítez, G.; Leonti, M. The historical development of pharmacopoeias and the inclusion of exotic herbal drugs with a focus on Europe and Brazil. *J. Ethnopharmacol.* **2019**, *240*, 111891. [[CrossRef](#)] [[PubMed](#)]
6. Calixto, J.B. The role of natural products in modern drug discovery. *An. Acad. Bras. Ciências* **2019**, *91* (Suppl. 3), e20190105. [[CrossRef](#)] [[PubMed](#)]
7. Uekane, T.M.; Nicolotti, L.; Griglione, A.; Bizzo, H.R.; Rubiolo, P.; Bicchi, C.; Rocha-Leão, M.H.; Rezende, C.M. Studies on the volatile fraction composition of three native Amazonian-Brazilian fruits: Murici (*Byrsonima crassifolia* L., Malpighiaceae), bacuri (*Platonia insignis* M., Clusiaceae), and sapodilla (*Manilkara sapota* L., Sapotaceae). *Food Chem.* **2017**, *219*, 13–22. [[CrossRef](#)]
8. Souza, A.C.; Alves, M.M.D.M.; Brito, L.M.; Oliveira, L.G.C.; Sobrinho-Júnior, E.P.C.; Costa, I.C.G.; Freitas, S.D.L.; Rodrigues, K.A.D.F.; Chaves, M.H.; Arcanjo, D.D.R.; et al. *Platonia insignis* Mart., a Brazilian Amazonian Plant: The Stem Barks Extract and Its Main Constituent Lupeol Exert Antileishmanial Effects Involving Macrophages Activation. *Evid. Based Complement. Altern. Med.* **2017**, *2017*, 3126458. [[CrossRef](#)]
9. Costa Júnior, J.S.; Ferraz, A.B.F.; Sousa, T.O.; Silva, R.A.; De Lima, S.G.; Feitosa, C.M.; Citó, A.M.; Melo Cavalcante, A.A.; Freitas, R.M.; Moura Sperotto, A.R.; et al. Investigation of biological activities of dichloromethane and ethyl acetate fractions of *Platonia insignis* Mart. seed. *Basic Clin. Pharmacol. Toxicol.* **2013**, *112*, 34–41. [[CrossRef](#)]
10. Rufino, M.D.S.M.; Alves, R.E.; de Brito, E.S.; Pérez-Jiménez, J.; Saura-Calixto, F.; Mancini-Filho, J. Bioactive compounds and antioxidant capacities of 18 non-traditional tropical fruits from Brazil. *Food Chem.* **2010**, *121*, 996–1002. [[CrossRef](#)]
11. de Freitas, F.A.; Araújo, R.C.; Soares, E.R.; Nunomura, R.C.S.; Silva, F.M.A.; Silva, S.R.S.; Souza, A.Q.L.; Souza, A.D.L.; Franco-Montalbán, F.; Acho, L.D.R.; et al. Biological evaluation and quantitative analysis of antioxidant compounds in pulps of the Amazonian fruits bacuri (*Platonia insignis* Mart.), ingá (*Inga edulis* Mart.), and uchi (*Sacoglottis uchi* Huber) by UHPLC-ESI-MS/MS. *J. Food Biochem.* **2018**, *42*, e12455. [[CrossRef](#)]
12. Coêlho, E.D.S.; Lopes, G.L.N.; Pinheiro, I.M.; Holanda, J.N.P.; Alves, M.M.M.; Carvalho Nogueira, N.; Carvalho, F.A.A.; Carvalho, A.L.M. Emulgel based on amphotericin B and bacuri butter (*Platonia insignis* Mart.) for the treatment of cutaneous leishmaniasis: Characterization and in vitro assays. *Drug Dev. Ind. Pharm.* **2018**, *44*, 1713–1723. [[CrossRef](#)]
13. da Silva, A.P.D.S.C.L.; Lopes, J.S.L.; Vieira, P.D.S.; Pinheiro, E.E.; da Silva, M.L.; Silva Filho, J.C.; da Costa, J.S., Jr.; David, J.M.; de Freitas, R. Behavioral and neurochemical studies in mice pretreated with garcinielliptone FC in pilocarpine-induced seizures. *Pharmacol. Biochem. Behav.* **2014**, *124*, 305–310. [[CrossRef](#)]
14. Lustosa, A.K.M.F.; Arcanjo, D.D.R.; Ribeiro, R.G.; Rodrigues, K.A.F.; Passos, F.F.B.; Piauilino, C.A.; Silva-Filho, J.C.; Araújo, B.Q.; Lima-Neto, J.S.; Costa-Júnior, J.S.; et al. Immunomodulatory and toxicological evaluation of the fruit seeds from *Platonia insignis*, a native species from Brazilian Amazon Rainforest. *Rev. Bras. Farmacogn.* **2016**, *26*, 77–82. [[CrossRef](#)]
15. Mei, B.; Chen, J.; Yang, N.; Peng, Y. The regulatory mechanism and biological significance of the Snail-miR590-VEGFR-NRP1 axis in the angiogenesis, growth and metastasis of gastric cancer. *Cell Death Dis.* **2020**, *11*, 241. [[CrossRef](#)]
16. Kong, H.; You, N.; Chen, H.; Teng, Y.S.; Liu, Y.G.; Lv, Y.P.; Mao, F.Y.; Cheng, P.; Chen, W.; Zhao, Z.; et al. Helicobacter pylori-induced adrenomedullin modulates IFN- $\gamma$ -producing T-cell responses and contributes to gastritis. *Cell Death Dis.* **2020**, *11*, 189. [[CrossRef](#)]
17. Kalange, M.; Nansunga, M.; Kasozi, K.I.; Kasolo, J.; Namulema, J.; Atusiimirwe, J.K.; Ayikobua, E.T.; Ssempijja, F.; Munanura, E.I.; Matama, K.; et al. Antimalarial combination therapies increase gastric ulcers through an imbalance of basic antioxidative-oxidative enzymes in male Wistar rats. *BMC Res. Notes* **2020**, *13*, 230.
18. Ahmed, O.A.A.; Fahmy, U.A.; Bakhaidar, R.; El-Moselhy, M.A.; Alfaleh, M.A.; Ahmed, A.F.; Hammad, A.S.A.; Aldawsari, H.; Alhakamy, N.A. Pumpkin Oil-Based Nanostructured Lipid Carrier System for Antiulcer Effect in NSAID-Induced Gastric Ulcer Model in Rats. *Int. J. Nanomed.* **2020**, *15*, 2529–2539. [[CrossRef](#)]
19. Abed, M.N.; Alassaf, F.A.; Jasim, M.H.M.; Alfahad, M.; Qazzaz, M.E. Comparison of Antioxidant Effects of the Proton Pump-Inhibiting Drugs Omeprazole, Esomeprazole, Lansoprazole, Pantoprazole, and Rabeprazole. *Pharmacology* **2020**, *105*, 645–651. [[CrossRef](#)]
20. Azmi, L.; Shukla, I.; Goutam, A.; Rao, C.V.; Jawaid, T.; Awaad, A.S.; Alqasoumi, S.I.; AlKhamees, O.A.; Kamal, M. Oxidative free radicals scavenging activity (in vitro and in vivo assay) of standardized fractions from the seeds of *Argyrea speciosa* (Chav-patta) a traditional Indian medicine. *Saudi Pharm. J. SPJ Off. Publ. Saudi Pharm. Soc.* **2019**, *27*, 1210–1215. [[CrossRef](#)]
21. Sokolova, O.; Naumann, M. Crosstalk Between DNA Damage and Inflammation in the Multiple Steps of Gastric Carcinogenesis. *Curr. Top. Microbiol. Immunol.* **2019**, *421*, 107–137.

22. Yanaka, A. Role of NRF2 in protection of the gastrointestinal tract against oxidative stress. *J. Clin. Biochem. Nutr.* **2018**, *63*, 18–25. [[CrossRef](#)]
23. Carneiro, J.G.; Holanda, T.D.B.L.; Quinderé, A.L.G.; Frota, A.F.; Soares, V.V.M.; Sousa, R.S.; Carneiro, M.A.; Martins, D.S.; Gomes Duarte, A.S.; Benevides, N.M.B. Gastroprotective Effects of Sulphated Polysaccharides from the Alga *Caulerpa mexicana* Reducing Ethanol-Induced Gastric Damage. *Pharmaceuticals* **2018**, *11*, 6. [[CrossRef](#)]
24. Mileva, M.; Dimitrova, A.; Krastev, D.; Alexandrova, A.; Tsvetanova, E.; Georgieva, A.; Galabov, A. Oseltamivir and S-Adenosyl-L-Methionine Combination as Effective Therapeutic Strategy for Suppression of Oxidative Damage in Lung Caused by Influenza Virus Infection in Mice. *Drug Res.* **2020**, *70*, 273–279. [[CrossRef](#)]
25. Queiroz, J.L.C.; Medeiros, I.; Piuvezam, G.; de França Nunes, A.C.; Gomes, C.C.; Maciel, B.L.L.; de Araújo Morais, A.H.; Passos, T.S. Effect of carotenoid encapsulation on antioxidant activities: A protocol for systematic review. *Medicine* **2020**, *99*, e19772. [[CrossRef](#)]
26. Zhu, Y.; Wu, Q.; Lv, H.; Chen, W.; Wang, L.; Shi, S.; Yang, J.; Zhao, P.; Li, Y.; Christopher, R.; et al. Toxicity of different forms of antimony to rice plants: Effects on reactive oxidative species production, antioxidative systems, and uptake of essential elements. *Environ. Pollut.* **2020**, *263*, 114544. [[CrossRef](#)]
27. Durazzo, A.; Lombardi-Boccia, G.; Santini, A.; Lucarini, M. Dietary Antioxidants and Metabolic Diseases. *Int. J. Mol. Sci.* **2021**, *22*, 12558. [[CrossRef](#)]
28. Genestra, M. Oxy radical radicals, redox-sensitive signalling cascades and antioxidants. *Cell. Signal.* **2007**, *19*, 1807–1819. [[CrossRef](#)]
29. Valko, M.; Leibfritz, D.; Moncol, J.; Cronin, M.T.D.; Mazur, M.; Telser, J. Free radicals and antioxidants in normal physiological functions and human disease. *Int. J. Biochem. Cell Biol.* **2007**, *39*, 44–84. [[CrossRef](#)]
30. Patlevič, P.; Vašková, J.; Švorc, P., Jr.; Vaško, L.; Švorc, P. Reactive oxygen species and antioxidant defense in human gastrointestinal diseases. *Integr. Med. Res.* **2016**, *5*, 250–258. [[CrossRef](#)]
31. Saha, S.; Roy, A.; Roy, K.; Roy, M.N. Study to explore the mechanism to form inclusion complexes of  $\beta$ -cyclodextrin with vitamin molecules. *Sci. Rep.* **2016**, *6*, 35764. [[CrossRef](#)]
32. Moorcroft, S.C.T.; Roach, L.; Jayne, D.G.; Ong, Z.Y.; Evans, S.D. Nanoparticle loaded hydrogel for the light-activated release and photothermal enhancement of antimicrobial peptides. *ACS Appl. Mater. Interfaces* **2020**, *12*, 24544–24554. [[CrossRef](#)]
33. Piazzini, V.; Landucci, E.; Urru, M.; Chiarugi, A.; Pellegrini-Giampietro, D.E.; Bilia, A.R.; Bergonzi, M.C. Enhanced dissolution, permeation and oral bioavailability of aripiprazole mixed micelles: In vitro and in vivo evaluation. *Int. J. Pharm.* **2020**, *583*, 119361. [[CrossRef](#)] [[PubMed](#)]
34. Alves Batista, F.; Brena Cunha Fontele, S.; Beserra Santos, L.K.; Filgueiras, L.A.; Nascimento, S.Q.; Sousa, J.M.C.; Gonçalves, J.C.R.; Mendes, A.N. Synthesis, characterization of  $\alpha$ -terpineol-loaded PMMA nanoparticles as proposed of therapy for melanoma. *Mater. Today Commun.* **2020**, *22*, 100762. [[CrossRef](#)]
35. Mendes, A.N.; Filgueiras, L.A.; Siqueira, M.R.P.; Barbosa, G.M.; Holandino, C.; de Lima Moreira, D.; Pinto, J.C.; Nele, M. Encapsulation of *Piper cabralanum* (Piperaceae) nonpolar extract in poly(methyl methacrylate) by miniemulsion and evaluation of increase in the effectiveness of antileukemic activity in K562 cells. *Int. J. Nanomed.* **2017**, *12*, 8363–8373. [[CrossRef](#)]
36. Souto, E.B.; Silva, G.F.; Dias-Ferreira, J.; Zielinska, A.; Ventura, F.; Durazzo, A.; Lucarini, M.; Novellino, E.; Santini, A. Nanopharmaceuticals: Part I-Clinical Trials Legislation and Good Manufacturing Practices (GMP) of Nanotherapeutics in the EU. *Pharmaceutics* **2020**, *12*, 146. [[CrossRef](#)]
37. Souto, E.B.; Silva, G.F.; Dias-Ferreira, J.; Zielinska, A.; Ventura, F.; Durazzo, A.; Lucarini, M.; Novellino, E.; Santini, A. Nanopharmaceuticals: Part II-Production Scales and Clinically Compliant Production Methods. *Nanomaterials* **2020**, *10*, 455. [[CrossRef](#)] [[PubMed](#)]
38. Yeung, A.W.K.; Souto, E.B.; Durazzo, A.; Lucarini, M.; Novellino, E.; Tewari, D.; Wang, D.; Atanasov, A.G.; Santini, A. Big impact of nanoparticles: Analysis of the most cited nanopharmaceuticals and nanonutraceuticals research. *Curr. Res. Biotechnol.* **2020**, *2*, 53–63. [[CrossRef](#)]
39. Arcanjo, D.D.R.; da Costa-Júnior, J.S.; Moura, L.H.P.; Ferraz, A.B.; Rossatto, R.R.; David, J.M.; Quintans-Júnior, L.J.; Oliveira, R.C.M.; Citó, A.M.G.L.; Oliveira, A.P. Garcinielliptone FC, a polyisoprenylated benzophenone from *Platonia insignis* Mart., promotes vasorelaxant effect on rat mesenteric artery. *Nat. Prod. Res.* **2014**, *28*, 923–927. [[CrossRef](#)]
40. Higuchi, T.; Connors, K.A. Phase solubility techniques. *Adv. Anal. Chem. Instrum.* **1965**, *4*, 207–212.
41. Coelho, L.N. Estudo da Inclusão de Filtros Solares em Ciclodextrinas e suas Aplicações em Dermocosmética. Master's Thesis, Faculdade de Farmácia do Rio de Janeiro, Rio de Janeiro, Brazil, 2001.
42. Costa Júnior, J.S.D.; Ferraz, A.D.B.F.; Feitosa, C.M.; Citó, A.M.D.G.L.; Saffi, J.; Freitas, R.M.D. Evaluation of effects of dichloromethane fraction from *Platonia insignis* on pilocarpine-induced seizures. *Rev. Bras. Farmacogn.* **2011**, *21*, 1104–1110. [[CrossRef](#)]
43. Weng, J.-R.; Tsao, L.-T.; Wang, J.-P.; Wu, R.R.; Lin, C.N. Anti-inflammatory phloroglucinols and terpenoids from *Garcinia subelliptica*. *J. Nat. Prod.* **2004**, *67*, 1796–1799. [[CrossRef](#)] [[PubMed](#)]
44. Weng, J.-R.; Lin, C.-N.; Tsao, L.-T.; Wang, J.P. Novel and anti-inflammatory constituents of *Garcinia subelliptica*. *Chemistry* **2003**, *9*, 1958–1963. [[CrossRef](#)]
45. Robert, A.; Nezamis, J.E.; Lancaster, C.; Hanchar, A.J. Cytoprotection by prostaglandins in rats. Prevention of gastric necrosis produced by alcohol, HCl, NaOH, hypertonic NaCl, and thermal injury. *Gastroenterology* **1979**, *77*, 433–443. [[CrossRef](#)]

46. Viana, A.F.S.C.; Lopes, M.T.P.; Oliveira, F.T.B.; Nunes, P.I.G.; Santos, V.G.; Braga, A.D.; Silva, A.C.A.; Sousa, D.P.; Viana, D.A.; Rao, V.S.; et al. (–)-Myrtenol accelerates healing of acetic acid-induced gastric ulcers in rats and in human gastric adenocarcinoma cells. *Eur. J. Pharmacol.* **2019**, *854*, 139–148. [[CrossRef](#)]
47. Ueda, S.; Okada, Y. Acid secretagogues induce Ca<sup>2+</sup> mobilization coupled to K<sup>+</sup> conductance activation in rat parietal cells in tissue culture. *Biochim. Biophys. Acta* **1989**, *1012*, 254–260. [[CrossRef](#)]
48. Ohkawa, H.; Ohishi, N.; Yagi, K. Assay for lipid peroxides in animal tissues by thiobarbituric acid reaction. *Anal. Biochem.* **1979**, *95*, 351–358. [[CrossRef](#)]
49. Geng, Q.; Li, T.; Wang, X.; Chu, W.; Cai, M.; Xie, J.; Ni, H. The mechanism of bensulfuron-methyl complexation with  $\beta$ -cyclodextrin and 2-hydroxypropyl- $\beta$ -cyclodextrin and effect on soil adsorption and bio-activity. *Sci. Rep.* **2019**, *9*, 1882. [[CrossRef](#)]
50. Chen, X.; Taguchi, T. Injectable inclusion complex composed of  $\alpha$ -cyclodextrin and hydrophobically modified poly(vinyl alcohol) as a cerebral aneurysm embolization material. *Polym. J.* **2020**, *52*, 793–802. [[CrossRef](#)]
51. Real, D.A.; Bolaños, K.; Priotti, J.; Yutronic, N.; Kogan, M.J.; Sierpe, R.; Donoso-González, O. Cyclodextrin-Modified Nanomaterials for Drug Delivery: Classification and Advances in Controlled Release and Bioavailability. *Pharmaceutics* **2021**, *13*, 2131. [[CrossRef](#)] [[PubMed](#)]
52. Fenyvesi, É.; Sohajda, T. Cyclodextrin-enabled green environmental biotechnologies. *Environ. Sci. Pollut. Res. Int.* **2022**, *29*, 20085–20097. [[CrossRef](#)] [[PubMed](#)]
53. Lima, P.S.S.; Lucchese, A.M.; Araújo-Filho, H.G.; Menezes, P.P.; Araújo, A.A.S.; Quintans-Júnior, L.J.; Quintans, J.S.S. Inclusion of terpenes in cyclodextrins: Preparation, characterization and pharmacological approaches. *Carbohydr. Polym.* **2016**, *151*, 965–987. [[CrossRef](#)] [[PubMed](#)]
54. Prodea, A.; Mioc, A.; Banciu, C.; Trandafirescu, C.; Milan, A.; Racoviceanu, R.; Ghiulai, R.; Mioc, M.; Soica, C. The Role of Cyclodextrins in the Design and Development of Triterpene-Based Therapeutic Agents. *Int. J. Mol. Sci.* **2022**, *23*, 736. [[CrossRef](#)] [[PubMed](#)]
55. Bouhadiba, A.; Rahali, S.; Belhocine, Y.; Allal, H.; Nouar, L.; Rahim, M. Structural and energetic investigation on the host/guest inclusion process of benzyl isothiocyanate into  $\beta$ -cyclodextrin using dispersion-corrected DFT calculations. *Carbohydr. Res.* **2020**, *491*, 107980. [[CrossRef](#)] [[PubMed](#)]
56. Ogawa, N.; Takahashi, C.; Yamamoto, H. Physicochemical characterization of cyclodextrin-drug interactions in the solid state and the effect of water on these interactions. *J. Pharm. Sci.* **2015**, *104*, 942–954. [[CrossRef](#)]
57. Aytac, Z.; Ipek, S.; Erol, I.; Durgun, E.; Uyar, T. Fast-dissolving electrospun gelatin nanofibers encapsulating ciprofloxacin/cyclodextrin inclusion complex. *Colloids Surf. B Biointerfaces* **2019**, *178*, 129–136. [[CrossRef](#)]
58. de Miranda, J.C.; Martins, T.E.A.; Veiga, F.; Ferraz, H.G. Cyclodextrins and ternary complexes: Technology to improve solubility of poorly soluble drugs. *Braz. J. Pharm. Sci.* **2011**, *47*, 665–681. [[CrossRef](#)]
59. Banjare, M.K.; Behera, K.; Banjare, R.K.; Pandey, S.; Ghosh, K.K. Inclusion complexation of imidazolium-based ionic liquid and  $\beta$ -cyclodextrin: A detailed spectroscopic investigation. *J. Mol. Liq.* **2020**, *302*, 112530. [[CrossRef](#)]
60. Gao, S.; Jiang, J.-Y.; Liu, Y.-Y.; Fu, Y.; Zhao, L.X.; Li, C.Y.; Ye, F. Enhanced Solubility, Stability, and Herbicidal Activity of the Herbicide Diuron by Complex Formation with  $\beta$ -Cyclodextrin. *Polymers* **2019**, *11*, 1396. [[CrossRef](#)]
61. Jansook, P.; Prajapati, M.; Pruksakorn, P.; Loftsson, T. Antifungal activity of econazole nitrate/cyclodextrin complex: Effect of pH and formation of complex aggregates. *Int. J. Pharm.* **2020**, *574*, 118896. [[CrossRef](#)]
62. Jansook, P.; Kurkov, S.V.; Loftsson, T. Cyclodextrins as solubilizers: Formation of complex aggregates. *J. Pharm. Sci.* **2010**, *99*, 719–729. [[CrossRef](#)] [[PubMed](#)]
63. Brewster, M.E.; Loftsson, T. Cyclodextrins as pharmaceutical solubilizers. *Adv. Drug Deliv. Rev.* **2007**, *59*, 645–666. [[CrossRef](#)] [[PubMed](#)]
64. Tripathi, P.K.; Gupta, S.; Rai, S.; Shrivatava, A.; Tripathi, S.; Singh, S.; Khopade, A.J.; Kesharwani, P. Curcumin loaded poly (amidoamine) dendrimer-plamitic acid core-shell nanoparticles as anti-stress therapeutics. *Drug Dev. Ind. Pharm.* **2020**, *46*, 412–426. [[CrossRef](#)] [[PubMed](#)]
65. Wei, M.; Yang, X.; Watson, P.; Yang, F.; Liu, H. A cyclodextrin polymer membrane-based passive sampler for measuring triclocarban, triclosan and methyl triclosan in rivers. *Sci. Total Environ.* **2019**, *648*, 109–115. [[CrossRef](#)]
66. Rama, A.C.R.; Veiga, F.; Figueiredo, I.V.; Sousa, A.; Caramona, M. Aspectos biofarmacêuticos da formulação de medicamentos para neonatos: Fundamentos da complexação de indometacina com hidroxipropil- $\beta$ -ciclodextrina para tratamento oral do fechamento do canal arterial. *Rev. Bras. Ciências Farm.* **2005**, *41*, 281–299. [[CrossRef](#)]
67. Nascimento, J.L.; Coêlho, A.G.; Barros, Y.S.O.; Silva, O.A.; Freitas, R.M.; Rocha, M.S.; David, J.M.; Costa Júnior, J.S.; Arcanjo, D.D.R.; Oliveira, R.C.M.; et al. Avaliação da atividade antioxidante in vitro do extrato hexânico da semente do bacuri (*Platonia insignis* Mart.) e de seu complexo de inclusão com  $\beta$ -ciclodextrina. *Bol. Inf. Geum* **2014**, *5*, 44–53.
68. Bezamat, J.M.; Yokaichiya, F.; Dias Franco, M.K.K.; Castro, S.R.; Paula, E.; Cabeça, L.F. Complexation of the local anesthetic pramoxine with hydroxypropyl-beta-cyclodextrin can improve its bioavailability. *J. Drug Deliv. Sci. Technol.* **2020**, *55*, 101475. [[CrossRef](#)]
69. Praphanwittaya, P.; Saokham, P.; Jansook, P.; Loftsson, T. Aqueous solubility of kinase inhibitors: II the effect of hexadimethrine bromide on the dovitinib/ $\gamma$ -cyclodextrin complexation. *J. Drug Deliv. Sci. Technol.* **2020**, *55*, 101463. [[CrossRef](#)]
70. Hu, X.; Zhou, Z.; Han, L.; Li, S.; Zhou, W. Preparation and characterization of phloretin by complexation with cyclodextrins. *New J. Chem.* **2020**, *44*, 5218–5223. [[CrossRef](#)]

71. Adeoye, O.; Conceição, J.; Serra, P.A.; Bento da Silva, A.; Duarte, N.; Guedes, R.C.; Corvo, M.C.; Aguiar-Ricardo, A.; Jicsinszky, L.; Casimiro, T.; et al. Cyclodextrin solubilization and complexation of antiretroviral drug lopinavir: In silico prediction; Effects of derivatization, molar ratio and preparation method. *Carbohydr. Polym.* **2020**, *227*, 115287. [[CrossRef](#)]
72. Somer, A.; Roik, J.R.; Ribeiro, M.A.; Urban, A.M.; Schoeffel, A.; Urban, V.M.; Farago, F.V.; Castro, L.V.; Sato, F.; Jacinto, C.; et al. Nystatin complexation with  $\beta$ -cyclodextrin: Spectroscopic evaluation of inclusion by FT-Raman, photoacoustic spectroscopy, and  $^1\text{H}$  NMR. *Mater. Chem. Phys.* **2020**, *239*, 122117. [[CrossRef](#)]
73. Ghosh, R.; Roy, K.; Subba, A.; Mandal, P.; Basak, S.; Kundu, M.; Roy, M.N. Case to case study for exploring inclusion complexes of an anti-diabetic alkaloid with  $\alpha$  and  $\beta$  cyclodextrin molecules for sustained dischargement. *J. Mol. Struct.* **2020**, *1200*, 126988. [[CrossRef](#)]
74. Tom, L.; Nirmal, C.R.; Dusthacker, A.; Magizhaveni, B.; Kurup, M.R.P. Formulation and evaluation of  $\beta$ -cyclodextrin-mediated inclusion complexes of isoniazid scaffolds: Molecular docking and in vitro assessment of antitubercular properties. *New J. Chem.* **2020**, *44*, 4467–4477. [[CrossRef](#)]
75. Celebioglu, A.; Uyar, T. Hydrocortisone/cyclodextrin complex electrospun nanofibers for a fast-dissolving oral drug delivery system. *RSC Med. Chem.* **2020**, *11*, 245–258. [[CrossRef](#)] [[PubMed](#)]
76. Zhou, L.; Liu, B.; Guan, J.; Jiang, Z.; Guo, X. Preparation of sulfobutylether  $\beta$ -cyclodextrin-silica hybrid monolithic column, and its application to capillary electrochromatography of chiral compounds. *J. Chromatogr. A* **2020**, *1620*, 460932. [[CrossRef](#)]
77. Banjare, M.K.; Banjare, R.K.; Behera, K.; Pandey, S.; Mundeja, P.; Ghosh, K.K. Inclusion complexation of novel synthesis amino acid based ionic liquids with  $\beta$ -cyclodextrin. *J. Mol. Liq.* **2020**, *299*, 112204. [[CrossRef](#)]
78. Yap, K.Y.L.; Chan, S.Y.; Lim, C.S. Infrared-based protocol for the identification and categorisation of ginseng and its products. *Food Res. Int.* **2007**, *40*, 643–652. [[CrossRef](#)]
79. Singh, G.; Singh, P.K. Complexation of a cationic pyrene derivative with sulfobutylether substituted  $\beta$ -cyclodextrin: Towards a stimulus-responsive supramolecular material. *J. Mol. Liq.* **2020**, *305*, 112840. [[CrossRef](#)]
80. Simsek, T.; Simsek, S.; Mayer, C.; Rasulev, B. Combined computational and experimental study on the inclusion complexes of  $\beta$ -cyclodextrin with selected food phenolic compounds. *Struct. Chem.* **2019**, *30*, 1395–1406. [[CrossRef](#)]
81. Paulino, P.H.S.; de Sousa, S.M.R.; Da Silva, H.C.; De Almeida, W.B.; Ferrari, J.L.; Guimarães, L.; Nascimento Júnior, C.S. A theoretical investigation on the encapsulation process of mepivacaine into  $\beta$ -cyclodextrin. *Chem. Phys. Lett.* **2020**, *740*, 137060. [[CrossRef](#)]
82. Bouchemela, H.; Madi, F.; Nouar, L. DFT investigation of host–guest interactions between  $\alpha$ -Terpineol and  $\beta$ -cyclodextrin. *J. Incl. Phenom. Macrocycl. Chem.* **2019**, *95*, 247–258. [[CrossRef](#)]
83. Yue, L.; Li, J.; Jin, W.; Zhao, M.; Xie, P.; Chi, S.; Lei, Z.; Zhu, H.; Zhao, Y. Host–guest interaction between 20(S)-protopanaxatriol and three polyamine-modified  $\beta$ -cyclodextrins: Preparation, characterization, inclusion modes, and solubilization. *J. Incl. Phenom. Macrocycl. Chem.* **2020**, *97*, 29–42. [[CrossRef](#)]
84. Li, J.; Chen, Q.; Zhang, S.; Jiang, Q.; Shang, J.; Zhou, L.; Li, Q.; Li, S.; Shi, S.; Li, Y.; et al. Maltosyl- $\beta$ -cyclodextrin mediated Supramolecular Host-Guest inclusion complex used for enhancing baicalin antioxidant activity and bioavailability. *J. Drug Deliv. Sci. Technol.* **2019**, *54*, 101346. [[CrossRef](#)]
85. Qiu, N.; Zhao, X.; Liu, Q.; Shen, B.; Liu, J.; Li, X.; An, L. Inclusion complex of emodin with hydroxypropyl- $\beta$ -cyclodextrin: Preparation, physicochemical and biological properties. *J. Mol. Liq.* **2019**, *289*, 111151. [[CrossRef](#)]
86. Osaki, M.; Takashima, Y.; Kamitori, S.; Yamaguchi, H.; Harada, A. X-ray crystal structures of  $\alpha$ -cyclodextrin–5-hydroxypentanoic acid,  $\beta$ -cyclodextrin–5-hydroxypentanoic acid,  $\beta$ -cyclodextrin– $\epsilon$ -caprolactone, and  $\beta$ -cyclodextrin– $\epsilon$ -caprolactam inclusion complexes. *J. Incl. Phenom. Macrocycl. Chem.* **2020**, *96*, 93–99. [[CrossRef](#)]
87. Gao, S.; Liu, Y.; Jiang, J.; Ji, Q.; Fu, Y.; Zhao, L.; Li, C.; Ye, F. Physicochemical properties and fungicidal activity of inclusion complexes of fungicide chlorothalonil with  $\beta$ -cyclodextrin and hydroxypropyl- $\beta$ -cyclodextrin. *J. Mol. Liq.* **2019**, *293*, 111513. [[CrossRef](#)]
88. Gao, S.; Jiang, J.; Li, X.; Liu, Y.; Zhao, L.; Fu, Y.; Ye, F. Enhanced physicochemical properties and herbicidal activity of an environment-friendly clathrate formed by  $\beta$ -cyclodextrin and herbicide cyanazine. *J. Mol. Liq.* **2020**, *305*, 112858. [[CrossRef](#)]
89. Aree, T.  $\beta$ -Cyclodextrin encapsulation of nortriptyline HCl and amitriptyline HCl: Molecular insights from single-crystal X-ray diffraction and DFT calculation. *Int. J. Pharm.* **2020**, *575*, 118899. [[CrossRef](#)]
90. Tambe, A.; Pandita, N.; Kharkar, P.; Niteshkumar, S. Encapsulation of boswellic acid with  $\beta$ - and hydroxypropyl- $\beta$ -cyclodextrin: Synthesis, characterization, in vitro drug release and molecular modelling studies. *J. Mol. Struct.* **2018**, *1154*, 504–510. [[CrossRef](#)]
91. Mura, P.; Bettinetti, G.P.; Cirri, M.; Maestrelli, F.; Sorrenti, M.; Catenacci, L. Solid-state characterization and dissolution properties of Naproxen–Arginine–Hydroxypropyl- $\beta$ -cyclodextrin ternary system. *Eur. J. Pharm. Biopharm.* **2005**, *59*, 99–106. [[CrossRef](#)]
92. Toropainen, T.; Velaga, S.; Heikkilä, T.; Matilainen, L.; Jarho, P.; Carlfors, J.; Lehto, V.P.; Järvinen, T.; Järvinen, K. Preparation of budesonide/ $\gamma$ -cyclodextrin complexes in supercritical fluids with a novel SEDS method. *J. Pharm. Sci.* **2006**, *95*, 2235–2245. [[CrossRef](#)] [[PubMed](#)]
93. Corti, G.; Capasso, G.; Maestrelli, F.; Cirri, M.; Mura, P. Physical–chemical characterization of binary systems of metformin hydrochloride with triacetyl- $\beta$ -cyclodextrin. *J. Pharm. Biomed. Anal.* **2007**, *45*, 480–486. [[CrossRef](#)] [[PubMed](#)]
94. Silva, D.M.; Martins, J.L.R.; de Oliveira, D.R.; Florentino, I.F.; da Silva, D.P.B.; Dos Santos, F.C.A.; Costa, E.A. Effect of allantoin on experimentally induced gastric ulcers: Pathways of gastroprotection. *Eur. J. Pharmacol.* **2018**, *821*, 68–78. [[CrossRef](#)] [[PubMed](#)]

95. Boligon, A.A.; de Freitas, R.B.; de Brum, T.F.; Waczuk, E.P.; Klimaczewski, C.V.; de Ávila, D.S.; Athayde, M.L.; de Freitas Bauermann, L. Antiulcerogenic activity of *Scutia buxifolia* on gastric ulcers induced by ethanol in rats. *Acta Pharm. Sin. B* **2014**, *4*, 358–367. [[CrossRef](#)] [[PubMed](#)]
96. Amaral, G.P.; de Carvalho, N.R.; Barcelos, R.P.; Dobrachinski, F.; Portella, R.L.; da Silva, M.H.; Lugokenski, T.H.; Dias, G.R.; da Luz, S.C.; Boligon, A.A.; et al. Protective action of ethanolic extract of *Rosmarinus officinalis* L. in gastric ulcer prevention induced by ethanol in rats. *Food Chem. Toxicol.* **2013**, *55*, 48–55. [[CrossRef](#)]
97. de Barros, M.P.; Lemos, M.; Maistro, E.L.; Leite, M.F.; Sousa, J.P.; Bastos, J.K.; Andrade, S.F. Evaluation of antiulcer activity of the main phenolic acids found in Brazilian Green Propolis. *J. Ethnopharmacol.* **2008**, *120*, 372–377. [[CrossRef](#)]
98. Santos, A.C.V.; Fernandes, C.C.; Lopes, L.M.; Sousa, A.H. Use of plant oils from the southwestern Amazon for the control of maize weevil. *J. Stored Prod Res* **2015**, *63*, 67–70. [[CrossRef](#)]
99. Da Silva, B.J.M.; Hage, A.A.P.; Silva, E.O.; Rodrigues, A.D.P. Medicinal plants from the Brazilian Amazonian region and their antileishmanial activity: A review. *J. Integr. Med.* **2018**, *16*, 211–222. [[CrossRef](#)]
100. Costa, J.S.; de Almeida, A.A.C.; Tomé, A.D.R.; Citó, A.M.G.L.; Saffi, J.; Freitas, R.M. Evaluation of possible antioxidant and anticonvulsant effects of the ethyl acetate fraction from *Platonia insignis* Mart. (Bacuri) on epilepsy models. *Epilepsy Behav.* **2011**, *22*, 678–684. [[CrossRef](#)]
101. Moonens, K.; Gideonsson, P.; Subedi, S.; Bugaytsova, J.; Romaõ, E.; Mendez, M.; Nordén, J.; Fallah, M.; Rakhimova, L.; Shevtsova, A.; et al. Structural Insights into Polymorphic ABO Glycan Binding by *Helicobacter pylori*. *Cell Host Microbe* **2016**, *19*, 55–66. [[CrossRef](#)]
102. Jaccob, A.A. Protective effect of N-acetylcysteine against ethanol-induced gastric ulcer: A pharmacological assessment in mice. *J. Intercult. Ethnopharmacol.* **2015**, *4*, 90–95. [[CrossRef](#)] [[PubMed](#)]
103. Soliman, N.A.; Zineldeen, D.H.; Katary, M.A.; Ali, D.A. N-acetylcysteine a possible protector against indomethacin-induced peptic ulcer: Crosstalk between antioxidant, anti-inflammatory, and antiapoptotic mechanisms. *Can. J. Physiol. Pharmacol.* **2017**, *95*, 396–403. [[CrossRef](#)] [[PubMed](#)]
104. Hegab, I.I.; Abd-Ellatif, R.N.; Sadek, M.T. The gastroprotective effect of N-acetylcysteine and genistein in indomethacin-induced gastric injury in rats. *Can. J. Physiol. Pharmacol.* **2018**, *96*, 1161–1170. [[CrossRef](#)] [[PubMed](#)]
105. Cabeza, J.; Motilva, V.; Martín, M.J.; de La Lastra, C.A. Mechanisms involved in gastric protection of melatonin against oxidant stress by ischemia-reperfusion in rats. *Life Sci.* **2001**, *68*, 1405–1415. [[CrossRef](#)]
106. Cássia Dos Santos, R.; Bonamin, F.; Périco, L.L.; Rodrigues, V.P.; Zanatta, A.C.; Rodrigues, C.M.; Sannomiya, M.; Dos Santos Ramos, M.A.; Bonifácio, B.V.; Bauab, T.M.; et al. Byrsonima intermedia A. Juss partitions promote gastroprotection against peptic ulcers and improve healing through antioxidant and anti-inflammatory activities. *Biomed. Pharmacother.* **2019**, *111*, 1112–1123. [[CrossRef](#)]
107. Magierowski, M.; Magierowska, K.; Hubalewska-Mazgaj, M.; Sliwowski, Z.; Pajdo, R.; Ginter, G.; Kwiecien, S.; Brzozowski, T. Exogenous and Endogenous Hydrogen Sulfide Protects Gastric Mucosa against the Formation and Time-Dependent Development of Ischemia/Reperfusion-Induced Acute Lesions Progressing into Deeper Ulcerations. *Molecules* **2017**, *22*, 295. [[CrossRef](#)]
108. Fagundes, F.L.; de Moraes Piffer, G.; Périco, L.L.; Rodrigues, V.P.; Hiruma-Lima, C.A.; Dos Santos, R.C. Chrysin Modulates Genes Related to Inflammation, Tissue Remodeling, and Cell Proliferation in the Gastric Ulcer Healing. *Int. J. Mol. Sci.* **2020**, *21*, 760. [[CrossRef](#)]
109. Milano, S.P.; Boucheix, O.B.; Reinheimer, T.M. Selepressin, a novel selective V(1A) receptor agonist: Effect on mesenteric flow and gastric mucosa perfusion in the endotoxemic rabbit. *Peptides* **2020**, *129*, 170318. [[CrossRef](#)]
110. Fanjul, C.; Barrenetxe, J.; De Pablo-Maiso, L.; Lostao, M.P. In vivo regulation of intestinal absorption of amino acids by leptin. *J. Endocrinol.* **2015**, *224*, 17–23. [[CrossRef](#)]
111. Menguy, R. Role of gastric mucosal energy metabolism in the etiology of stress ulceration. *World J. Surg.* **1981**, *5*, 175–180. [[CrossRef](#)]
112. Andrews, F.J.; Malcontenti-Wilson, C.; O'Brien, P.E. Polymorphonuclear leukocyte infiltration into gastric mucosa after ischemia-reperfusion. *Am. J. Physiol.* **1994**, *266*, G48–G54. [[CrossRef](#)] [[PubMed](#)]
113. Wada, K.; Kamisaki, Y.; Kitano, M.; Kishimoto, Y.; Nakamoto, K.; Itoh, T. A new gastric ulcer model induced by ischemia-reperfusion in the rat: Role of leukocytes on ulceration in rat stomach. *Life Sci.* **1996**, *59*, PL295–PL301. [[CrossRef](#)] [[PubMed](#)]
114. Kitano, M.; Bernsand, M.; Kishimoto, Y.; Norlén, P.; Håkanson, R.; Haenuki, Y.; Kudo, M.; Hasegawa, J. Ischemia of rat stomach mobilizes ECL cell histamine. *Am. J. Physiol. Gastrointest. Liver. Physiol.* **2005**, *288*, G1084–G1090. [[CrossRef](#)] [[PubMed](#)]
115. Aboul Naser, A.; Younis, E.; El-Feky, A.; Elbatany, M.; Hamed, M. Management of *Citrus sinensis* peels for protection and treatment against gastric ulcer induced by ethanol in rats. *Biomarkers* **2020**, *25*, 349–359. [[CrossRef](#)]
116. Ahmed, I.; Elkablawy, M.A.; El-Agamy, D.S.; Bazarbay, A.A.; Ahmed, N. Carvedilol safeguards against aspirin-induced gastric damage in rats. *Hum. Exp. Toxicol.* **2020**, *39*, 1257–1267. [[CrossRef](#)]

117. Doğan, G.; İpek, H. The protective effect of *Ganoderma lucidum* on testicular torsion/detorsion-induced ischemia-reperfusion (I/R) injury. *Acta Cir. Bras.* **2020**, *35*, e202000103. [[CrossRef](#)]
118. Liu, R.; Hao, Y.-T.; Zhu, N.; Liu, X.R.; Kang, J.W.; Mao, R.X.; Hou, C.; Li, Y. The Gastroprotective Effect of Small Molecule Oligopeptides Isolated from Walnut (*Juglans regia* L.) against Ethanol-Induced Gastric Mucosal Injury in Rats. *Nutrients* **2020**, *12*, 1138. [[CrossRef](#)]

**Disclaimer/Publisher's Note:** The statements, opinions and data contained in all publications are solely those of the individual author(s) and contributor(s) and not of MDPI and/or the editor(s). MDPI and/or the editor(s) disclaim responsibility for any injury to people or property resulting from any ideas, methods, instructions or products referred to in the content.